Holistic approach for microgrid planning for e-mobility infrastructure under consideration of long-term uncertainty

Muhammad Tayyab[*,1], *Ines Hauer*[2], *Sebastian Helm*[3]
[1]*Fundamental Electrochemistry (IEK-9), Institut für Energie- und Klimaforschung, Forschungszentrum Jülich*
[2]*Institut für Elektrische Energietechnik und Energiesysteme, Technische Universität Clausthal*
[3]*Chair Electric Power Networks and Renewable Energy (LENA), Otto von Guericke University Magdeburg, Germany*
[*] *m.tayyab@fz-juelich.de*

Abstract

Integrating renewable energy sources in sectors such as electricity, heat, and transportation has to be planned economically, technologically, and emission-efficient to address global environmental issues. Microgrids appear to be the solution for large-scale renewable energy integration in these sectors. The microgrid components must be optimally planned and operated to prevent high costs, technical issues, and emissions. Existing approaches for optimal microgrid planning and operation in the literature do not include a solution for e-mobility infrastructure development. Consequently, the authors provide a compact new methodology that considers the placement and the stochastic evolution of e-mobility infrastructure. In this new methodology, a retropolation approach to forecast the rise in the number of electric vehicles, a monte-carlo simulation for electric vehicle (EV) charging behaviors, a method for the definition of electric vehicle charging station (EVCS) numbers based on occupancy time, and public EVCS placement based on monte-carlo simulation have been developed. A deterministic optimization strategy for the planning and operation of microgrids is created using the abovementioned methodologies, which additionally consider technical power system issues. As the future development of e-mobility infrastructure has high associated uncertainties, a new stochastic method referred to as the information gap decision method (IGDM) is proposed. This method provides a risk-averse strategy for microgrid planning and operation by including long-term uncertainty related to e-mobility. Finally, the deterministic and stochastic methodologies are combined in a novel holistic approach for microgrid design and operation in terms of cost, emission, and robustness.

The proposed method has been tested in a new settlement area in Magdeburg, Germany, under three different EV development scenarios (negative, trend, and positive). EVs are expected to reach 31 percent of the total number of cars in the investigated settlement area. Due to this, three public electric vehicle charging stations will be required in the 2031 trend scenario. Thus, the investigated settlement area requires a total cost of 127,029 €. In association with possible uncertainties, the cost of the microgrid must be raised by 80 percent to gain complete robustness against long-term risks in the development of EVCS.

Keywords: Electric vehicle charging station, Electric vehicle, monte-carlo simulation, Information gap decision method, E-mobility infrastructure, Holistic approach, optimizations, sector coupling

Nomenclature							
parameters				**Variables and indices**			
EV	*Electric vehicle*	N_{EV}	*Number of EVs*	P_{elec}	*Power consumed by electrolyser*	C_p	*Betz value*
EVCS	*Electric vehicle charging station*	X_o	*Number of EVs in the initial year*	$P_{\mathrm{HP,in}}$	*Power consumed by heat pump*	ν	*Wind speed*
IGDM	*Information gap decision method*	$\mathcal{M}$	*EV rising rate*	P_{EVCS}	*Power consumed in EVCS*	η_M	*Solar module efficiency*
ICE	*Internal combustion engines*	τ	*Difference between the current year and the initial year*	P_{DERs}	*DERs power*	P_{in}	*Active power injected*
CHP	*Combined heat and power*	$soc_{EV,t}$	*State of charge of the EV battery*	$P_{DERs,cap}$	*Power capacity of DERs*	$\boldsymbol{A}$	*Connecting matrix away from nodes*
PV	*Photovoltaic*	$E_{\mathrm{cons,\ tr}}$	*Energy consumption of the EV during the time of travel (tr)*	$P_{DERs,max}$	*Power capacity limit of DERs*	$\boldsymbol{B}$	*Connecting matrix into nodes*
EESS	*Electrical energy storage system*	$E_{\mathrm{EV,bat}}$	*Rated capacity of the battery of the electric vehicle*	$P_{ES,cap}$	*Power capacity of Energy storage systems*	I_n	*Branch current*
TESS	*Thermal energy storage system*	P_{EVCS}	*Rated power of EVCS*	$P_{ES,ch}$	*Charge power of Energy storage systems*	P_{s}	*Branch active power*
P2H	*Power to hydrogen*	i, j	*Nodes of the microgrid*	γ_1, γ_2	*Binary variable*	R_{n}	*Resistance of the branch*
RES	*Renewable energy sources*	$NVSI_{\mathrm{i}}$	*NVSI for a node number (i)*	$P_{ES,disch}$	*Power capacity limit of Energy storage systems*	Q_{in}	*Reactive power injected*
DIN	*Deutsche Institut für Normung e.V.*	U_k	*Nominal voltage*	E_{ES}	*Energy of Energy storage systems*	Q_s	*Branch reactive power*
VDI	*Verein Deutscher Ingenieure e.V.*	U_j	*Voltage at the j^{th} node*	η_{ES}	*Energy storage systems efficiencies*	X_{n}	*Reactance of the branch*

CO2	*Carbon dioxide*	n	*Total number of nodes*	$Q_{\mathrm{HP,out}}$	*Heat generated by heat pump*	v_n	*Voltage after assumption*
DERs	*Distributed energy resources*	Y	*Planning horizon*	$SCOP_{HP}$	*SCOP of heat pump*	l_{max}	*Thermal limit of cable*
NVSI	*Node voltage-sensitive index*	C_{inv}	*Investment cost*	$P_{w,n}$	*Normalized power generated by wind system*	Γ	*Uncertainty set*
HESS	*Hydrogen energy storage system*	C_{op}	*Operational cost*	P_{Irr}	*Irradiance*	α_{EVCS}	*Uncertainty region*
HP	*Heat pump*	$C_{\mathrm{penalty,\ CO2}}$	*CO_2 penalty cost*	$H_{2,out}$	*Hydrogen produced*	N_{EVCS}	*number of EVCS*
GHG	*Greenhouse gasses*	EM_{grid}	*Grid emission intensity parameter*	H_{low}	*Lower heating value of hydrogen*	$\widehat{N}_{EVCS}$	*Uncertain number of EVCS*
SFH	*Single family house*	C_{EM}	*Cost of CO2 emission*	Q_{FC}	*Heat produced by fuel cell*		
MFH	*Multi-family house*	t	*Operational horizon*	Θ_{FC}	*Heating efficiency of fuel cell*	f_b	*allowed budget*
CRE	*Commercial real estate*	P_{PV}	*Power generated by PV systems*	ρ	*Density*		
PCC	*Point of common coupling*	P_w	*Power generated by wind system*	A_w	*Rotor area*		
KBA	*Kraftfahrt-Bundesamt*	P_{grid}	*Power imported from grid*				
SCOP	*Seasonal coefficient of performance*	P_{BD}	*Battery discharge*				
kW	*Kilowatt*	P_{FC}	*Power generated by fuel cell*				
mm	*Millimeter*	P_{Load}	*Electrical load*				
kV	*Kilovolt*	P_{BC}	*Battery discharge*				
MVA	*Megavolt-amperes*						
m^3	*Cubic meter*						
Min	*Minimization*						
Max	*Maximization*						

1 Introduction

Germany aims to be an emission-free country by 2045 [1]. Greenhouse gases are targeted to be reduced by at least 65 percent by 2030 and 88 percent by 2040 compared to 1990 levels [2]. Renewable energy sources must replace fossil fuels in all sectors to achieve these emissions reduction targets. The primary GHG emissions in the transport sector are caused by internal combustion engines (ICE). Because of the depletion of fossil fuels, the usage of ICE encourages carbon dioxide emissions that contribute to global warming. In the long-term, ICE will be replaced by lower-emission or zero-emission vehicles, such as hybrid, electric, and fuel-cell vehicles [3]. A high amount of electric vehicles require a significant amount of charging energy. Therefore, a substantial proportion of renewable energy sources must power the e-mobility infrastructure. The local renewable energy generation to support the e-mobility infrastructure will be emission-effective.

Consequently, to plan for a secure local renewable supply to e-mobility infrastructure, the growth in the number of EVs and EVCS must be estimated. Furthermore, the low-voltage grid usually powers the EVCS and EVs. Furthermore, installed renewables such as PV are mostly integrated into the middle and low voltage grid [4]. However, the existing power grid will not always be able to handle the additional power and adverse impacts due to the large-scale deployment. A microgrid can be a solution for integrating many renewable energy sources and e-mobility infrastructure in a low-voltage grid. Nevertheless, the components must be optimally planned to avoid high costs, technical problems, and high emissions. Motivated by the alternatives to power the sustainable e-mobility infrastructure alongside other demands, optimal microgrid planning and operation are needed. The best planning and operation can be realized for a new settlement area where sustainable energy and power supply may be developed for a green, efficient, and intelligent infrastructure-based community.

A microgrid's decision-making must be planned for the future, considering affecting variables. Furthermore, the investment in the microgrid needs to be backed up by confidence in smooth and secure operation. An overestimated microgrid is a waste of money, whereas underestimated one has issues such as high energy import from the conventional grid. Optimization algorithms solve these problems with optimal planning and operation of the microgrid. Uncertain or unavailable data that are needed to estimate the future effect of microgrids for decision-making are the major hurdles in efficient microgrid planning and operation. Significantly, e-mobility infrastructure development has been fraught with long-term uncertainties. The following points address the risks associated with the e-mobility infrastructure:

- Long-term uncertainty: The increase in the number of EVCS is influenced by direct and indirect factors. Some of the determining elements are listed below.
  - Direct factor
    - The rise in the number of EVs
  - Indirect factors
    - Development of EV battery technology
    - Development of charging point technology
    - Developments in the government regulation
    - Development of public infrastructure
    - Announcements of electric vehicle subsidies
    - Political infrastructure goals
    - Development of other alternative transport technologies, such as synthetic fuels and fuel cell vehicles

Due to these factors, microgrid planning and operation need to consider long-term uncertainty regarding e-mobility infrastructure. The different scenarios show that the forecasts are based on past experiences. However, the number of EVCS can be triggered toward positive or negative due to the direct and indirect influencing factors. For that reason, the forecast has a long-term uncertainty that needs to be modeled for a risk-averse situation in microgrid decision-making.

The optimal microgrid planning and operation have been studied vastly. Microgrid planning and operation considering loads, renewables, and energy storage are proposed in [5,6]. These studies include energy storage and demand responses for the promotion of renewables and cost reduction. Furthermore, the multi-energy microgrid to optimize the portfolio mix for the components is proposed in [7,8]. In this study, generation units such as combined heat and power (CHP), photovoltaic (PV), and wind systems are alongside the energy storage units such as electrical energy storage system (EESS) and thermal energy storage system (TESS) to satisfy the electrical and heat demand. The power-to-heat (P2H) sector coupling complements the analysis. Renewable energy-based power to hydrogen (P2H) technology uses renewable energy sources (RES) to generate valuable heat energy for consumers to decrease curtailments [9]. The studies neglect the e-mobility sector, especially the inclusion of EVCS as an additional electrical load in the planning and operation horizon.

However, in [10-12], the electrical vehicle charging load is generally shown by a probability distribution and has been included as a unified aggregator. This approach will lead to an unreal realization of e-mobility infrastructure planning as the EV load and the number of EVCS are interdependently independent. Due to this, the question of how many EVCS are sufficient for how many EVs is raised. Hence, the number of EVs and EVCS in a community is an important problem for planning and operation. Apart from the number of EVCS, the placement of EVCS is also crucial due to the high load associated.

The authors of [13] present an optimization process for optimal siting and sizing with road networks using graph theory. A genetic optimization-based algorithm considering cost, EV energy losses, and power system losses has been presented [14]. An EVCS placement algorithm has been shown for under-construction traffic networks by minimizing transportation waste costs using queuing theory [15]. A heuristic planning method considering the EVs charging demand rather than the traffic model has been present in [16]. The authors of [17] developed a location model considering an EV driver's existing activities. While a colony optimization has been presented for optimal placement considering cost, real power loss, voltage instability, and traffic flow constraints in [18-20]. A particle swarm optimization (PSO) has shown a better and faster convergence for this problem in [21-23]. Algorithms such as genetic algorithms (GA) and teaching-learning-based algorithms have also been used for this problem in [24-31]. In addition to heuristic techniques, the primal-dual interior-point algorithm has been used to find the optimal location depending on coverage and environmental factors [32]. Greedy algorithms and linear programming have also been used for this issue in [33,34]. In the above-stated methods, the multi-period planning for the development in the e-mobility sector, e.g., the rise in the number of EVs and EVCS, the realistic random behavior of EV depending on the traffic model is still lacking to the best of the author's knowledge. Furthermore, in a planning problem, the placement for EVCS is probabilistic due to the high number of impacting factors, such as the electrical grid structure, space, accessibility, and the quantity of EVs expected to be charged. The field of e-mobility development modeling has benefited from the approaches below to take the impacts mentioned earlier into account.

- ❖ Model for e-mobility infrastructure
    - o Forecast method for the number of EVs based on retropolation and extrapolation
    - o Monte-carlo simulation for the EVs charging behavior
    - o The determination of the number of EVCS based on the occupancy time
    - o EVCS placement algorithm based on monte-carlo simulation

Although the above-stated method considers planning and operation for mix-portfolio for DERs, these are solved without any uncertainty or just short-term uncertainties. However, the long-term uncertainty has not been considered. A study that evaluated long-term uncertainties regarding the declining cost of the battery is solved with robust optimization [35]. The long-term uncertainties regarding the rise in the EVCS are still lacking. To reduce the financial, emission, and technical risks, novel approaches are needed considering the surge in EVCS uncertainty.

The study developed a new robust decision-making method for microgrids in a new settlement area. The proposed method is a risk-averse stochastic optimal microgrid planning method considering the long-term uncertainty. The risk-averse levels then enable the decision-makers to decide on the microgrid planning and operation based on robustness for long-term uncertainty. The contributed methods developed for the stochastic microgrid planning and operation are as follows:

- ❖ A new information gap decision method (IGDM) is developed for optimal microgrid planning under the rise in EVCS uncertainties.

Finally, a holistic approach that combines the deterministic and stochastic optimization approach enables the planning and operation of a microgrid optimally. The proposed combined approach is claimed to be beneficial for decision-makers to increase the local use of renewables when the e-mobility develops with associated uncertainties.

The paper is organized as follows. The methodology is described in section 2. Firstly, in this section, the e-mobility infrastructure modeling methodology is presented. Secondly, the formulation for the optimization method is given, consisting of a deterministic and stochastic optimization model. Finally, in section 3, the results are discussed, and a conclusion with an outlook is given in section 4.

2 Methodology

The study aims to optimally plan and operate a microgrid that can be built with existing electrical grid infrastructure. The microgrid is assumed to be a radial low-voltage grid consisting of connection nodes, lines, a transformer, and loads. The line parameters are modeled as NAYY 4x 35-150 mm², while the house connections are depicted as NAYY 4x 16-50 mm² [36,37]. The transformer is a 15 kV/0.4 kV transformer with a rating of 0.63 MVA. Different types of loads are considered, such as single-family houses, multi-family houses, and commercial real estate. The nominal line-to-line voltage for the electric low-voltage grid is 400 V [38], and the voltage must be in the range of ±10 percent of the nominal voltage according to DIN-EN-50160 [39] during the total planning period, maintaining the microgrid's secure operation and customer satisfaction.

A microgrid also has an associated heating demand. The heating demand is computed using VDI4655 [40]. The proposed methodology consists of two parts. In the first part, the e-mobility infrastructure is modeled. Secondly, the deterministic and stochastic optimization model is prepared with the component model and input parameters. Microgrid planning and optimization are based on a novel concept for the growth of e-mobility infrastructure. The

parameter value and the initial conditions define the model's output in deterministic models. The stochastic model considers uncertainties, meaning that the same set of parameter values and initial conditions will produce distinct outcomes. After the input parameters, such as electrical and heat loads, are modeled, the e-mobility infrastructure is determined. The holistic approach combining e-mobility infrastructure deterministic and stochastic optimization model is proposed for planning a new settlement area, as shown in figure 2.1. A pseudo-code for the Holistic methodology is given in the annex.

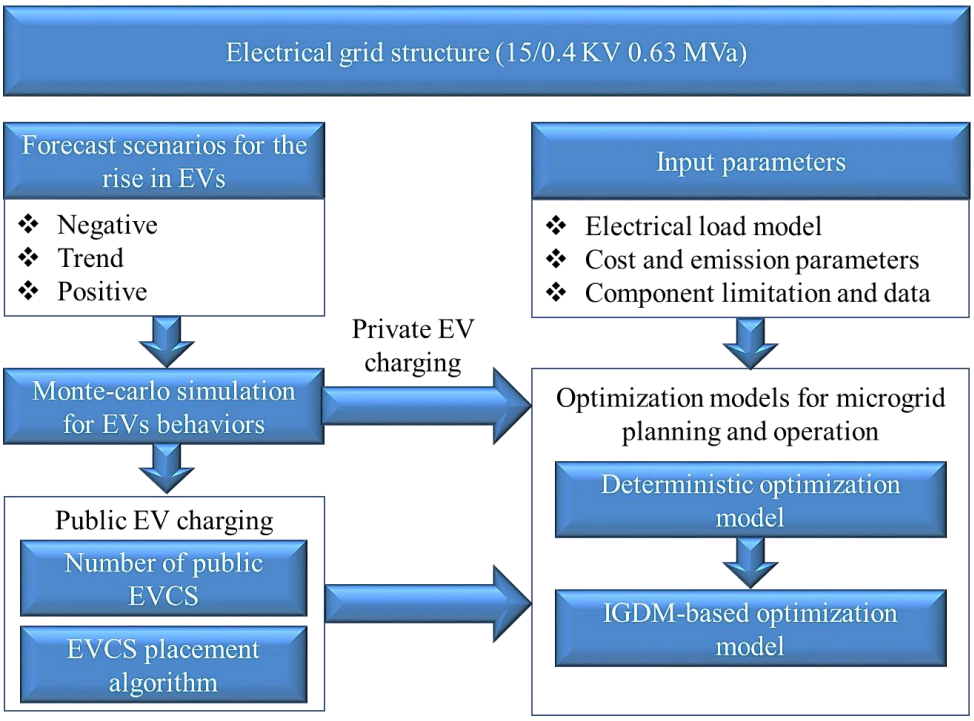

Figure 2.1 Microgrid proposed methodology

2.1 E-mobility infrastructure

The modeling of e-mobility infrastructure is performed in three steps. First, the rise in EVs is forecasted for different scenarios. The number of EVCS is modeled based on the increase in EVs and charging behavior, considering occupancy duration. Finally, a placement algorithm is incorporated to find the best place for the number of EVCS. A pseudo-code for the methodology of e-mobility infrastructure is given in the annex.

2.1.1 Forecast for the rise in the number of EVs based on retropolation

The first step is to develop a future scenario for the number of EVs based on generated scenarios shown in figure 2.1. The number of EVs is essential to decide the number of EVCS. The critical factor is to define the realization of these scenarios consistently and completely. It is assumed that the development of EVs over conventional vehicles depends on the investment cost, operational cost, driving benefit, and additional benefits.

Investment cost

> **Negative**: *The assumed cost targets are not reached. in 2026, electric vehicles will be even more expensive than ICE. The federal government did not extend the funding (poor costs/benefits; more investments in public transport or other technologies)*

Trend: *Production costs fall through technology improvements, learning, and economies of scale, especially battery prices. It is expected that the assumed cost parity will be reached by 2026. Around 300,000 vehicles are to be subsidized.*

Positive: *The assumed cost targets reach much earlier (e.g., 2024). Therefore, cost advantages will be achieved in 2026. The federal government continues to subsidize vehicles to accelerate the turnaround in traffic*

Operational cost

Negative: *Energy costs rise, CO_2 tax rises moderately, and vehicle tax is levied. Insurance and repairs are a little more expensive as compared to ICE.*

Trend: *Energy costs rise despite lower production costs for renewables, and vehicle tax remains exempt for ten years. The advantage of CO_2 tax increases (higher CO_2 prices with a simultaneous reduction in CO_2 intensity of electricity). Insurance, wear and tear, and repairs are also not so expensive.*

Positive: *Energy costs decreases. CO_2 tax rises dynamically, and vehicle tax exemption remains. Insurance and repairs become cheaper based on empirical values*

Driving benefits

Negative: *For efficiency, acceleration and driving experience is not further developed. Driving range, mileage, and charging time remains low.*

Trend: *There are no significant developments in acceleration. The driving range is increasing continuously, more and more fast-charging stations are being set up, and charging time is approaching a vehicle tank duration.*

Positive: *Acceleration and driving experience increase to a more precise distance than combustion engines. Excellent driving range as compared to combustion engines. Charging (e.g., by induction) takes place without additional effort.*

Other benefits

Negative: *Space is only slightly better in EVs. Similar features to ICE in terms of storage. The number of variants remains lower than combustion engines*

Trend: *Space is increasing moderately through further optimizations. Equipment is becoming more extensive, and it is growing in importance for bi-directional charging. A variety of variants is developed as compared to combustion engines*

Positive: *Significantly more space and better equipment in all EVs. EVs are far better in terms of storage. The variety of variants exceeds combustion engines*

A trend is identified through literature for each of these factors, and the development of trend scenarios is estimated. The positive and negative scenarios are then computed by shifting the value of the key parameters. Based on the key factors, the scenario development compared to the conventional vehicle is shown in table [41].

Table 2.1 assessment of the key factor to generate scenario for 2026

Key factors	Positive	Trends	Negative
Investment cost	EV better	EV neutral	EV worse
Operational cost	EV much better	EV better	EV marginal better
Driving benefit	EV better	EV neutral	EV worse
Another benefit	EV better	EV neutral	EV marginal better
Assumed EV share	55%	40%	20%

Table 2.1 illustrates how EVs outperforms traditional vehicle. These assumptions rebased on the EVs registered. The EVs will be bought and registered more if better in these factors. The assumed EV shares are based on the study's hypothesis [42]. Due to this, these shares can be flexible to be changed. The percentage of EVs must be assumed in 2026 to implement retropolation for the following five years. The share of EVs compared to conventional vehicles in 2026 is known from table 2.1. Once the number of EVs in 2026 is known, the number from 2022 to 2026 is developed through retropolation. Retropolation is the technique to connect the future with the current scenarios shown in figure 2.2 [43]. The meaningful trend analysis leads to planning the future through retropolation.

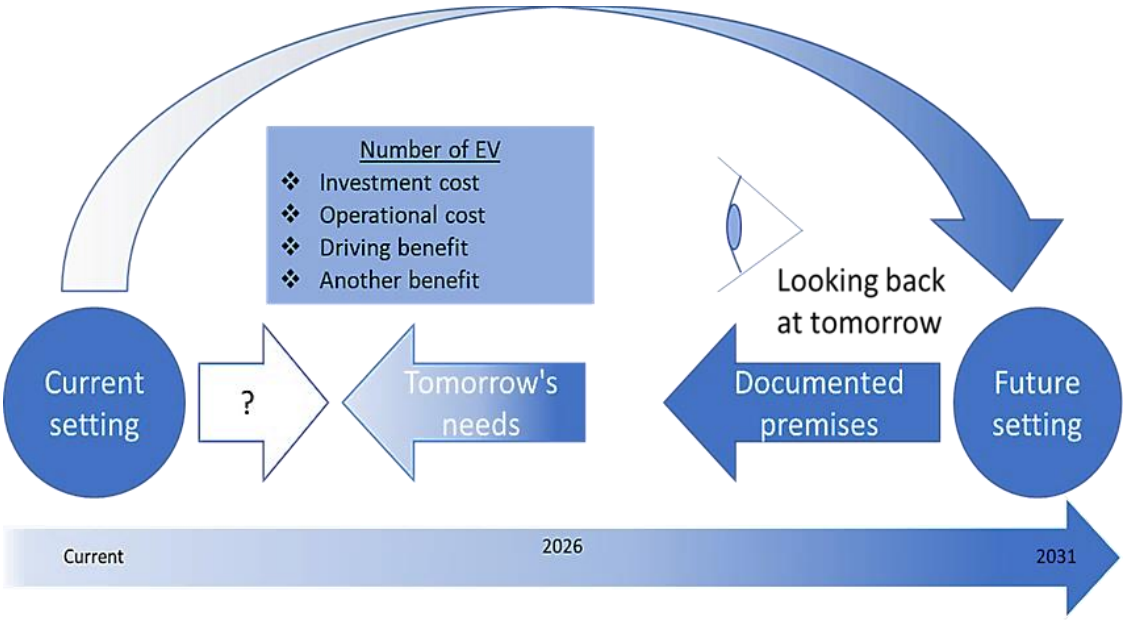

Figure 2.2 Retropolation method

The forecast for the number of EVs is considered to grow exponentially due to user adoption. Due to this, the exponential growth function for the rise in the number of EVs (N_{EV}) in a year (y) in the planning horizon is shown in (2.1).

$$N_{\mathrm{EV}} = X_{\mathrm{o}}(\mathcal{M})^{\tau} \tag{2.1}$$

where X_{o} is the number of EVs in the initial year. τ is the difference between the current year and the initial year. The initial year is considered to be 2021 in the present study, and the current year will be changing on the planning horizon. $\mathcal{M}$ is the rate at which the rise of the EVs can reach 20 percent for negative, 40 percent for trend, and 55 percent for the positive scenario in 2026. The value of $\mathcal{M}$ is taken from the study [41].

2.1.2 Electric vehicle behavior using monte-carlo simulation

The EVs can be in three different states (traveling, charging, or parked without charging). Due to the EV owner's random decision parameters, predicting these states at any given time step is nearly impossible. Parameters such as the number of trips, arrival time, departure time, kilometers traveled in a trip, duration of a trip, and power consumption according to speed are some of the EV owner's arbitrary decisions. Due to this, these parameters must be considered as random as much as possible. The monte-carlo simulation is used to model the EV behaviors and evaluate randomness.

Nonetheless, examining as many random variables as possible regarding EV behaviors would be preferable. Still, some of them must be fixed to avoid high complexities. The characteristics such as the number of trips, power cost per kilometer, and minimum EV battery state of charge required before departure are regarded as fixed parameters in the current studies. The arrival times, kilometers traveled, and travel duration is assumed to follow a distribution. The distribution has resulted chiefly from a detailed traffic model of Burg city in Germany. The current study uses the Burg traffic model's survey data for the probability distribution fit in the monte-carlo simulation [44,41]. Based on the Burg traffic model, the EVs arrival distribution is distinguished for each district type. The traffic data must be fitted with the available probability distribution functions to simulate the EV load based on these parameters. For a settlement area classified as a residential area with a small number of shops and markets, the following distribution function and related distribution fit are displayed in figure 2.2. It is assumed that 15 percent of the time, the EVs will charge from public EVCS [45].

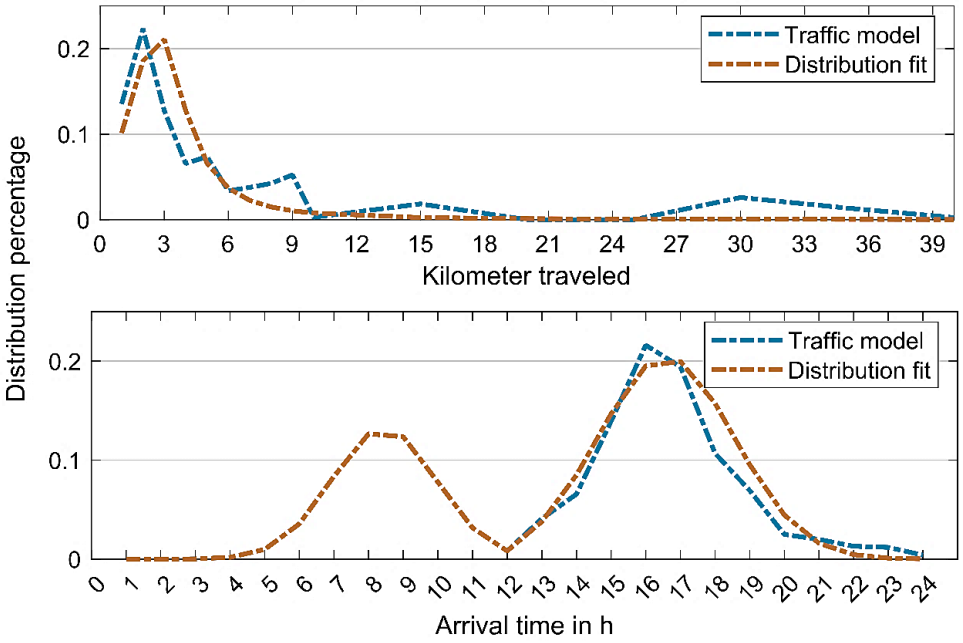

Figure 2.2 Traffic model and distribution fit for a residential area [41,44,46]

The precise EVs that will charge from private and public charging stations are picked randomly. The ratio between the number of EVs and nodes in the grid is used to deploy the private charging stations. The distribution of private charging stations in the electrical network is linear and even, with a ratio determined by the total number of (anticipated) electric vehicles and network connection nodes. If the ratio of the number of EVs to the total nodes is n, a private EV charging station with a rated power of 11 kW will be placed in every nth node of the grid. The nodes can have more than one private charging station depending on the number of EVs and the available grid nodes. When traveling, the change in the state of charge of the EV battery (soc_{EV}) is calculated as given in (2.2), where E_{cons} is the energy consumption of the EV during the time of travel (tr).

$$soc_{\mathrm{EV},t} = soc_{\mathrm{EV},t-1} - \frac{E_{\mathrm{cons},\,tr}}{E_{\mathrm{EV,bat}}} \tag{2.2}$$

Here, $E_{\mathrm{EV,bat}}$ is the rated capacity of the battery of the electric vehicle. The energy consumption of an EV is calculated by multiplying the consumption per kilometer and kilometer traveled. A value of 0.1922 kWh per kilometer has been used [41]. If the soc_{EV} during the charging state is smaller than 0.9, the EV is charged with a rated power of EVCS (P_{EVCS}). The EVs are charged until the charging time (t_{ch}) or soc_{EV}=1 is reached. A 22 kW EVCS is assumed in the present study for public charging, and 11 kW is used for private charging. At the time of charging, the soc_{EV} is determined according to (2.3).

$$soc_{\mathrm{EV},t} = soc_{\mathrm{EV},\,t-1} + \frac{P_{\mathrm{EVCS}}\, t_{\mathrm{ch}}}{E_{\mathrm{EV,\,bat}}} \tag{2.3}$$

The EV behavior simulation method is given in figure 2.3.

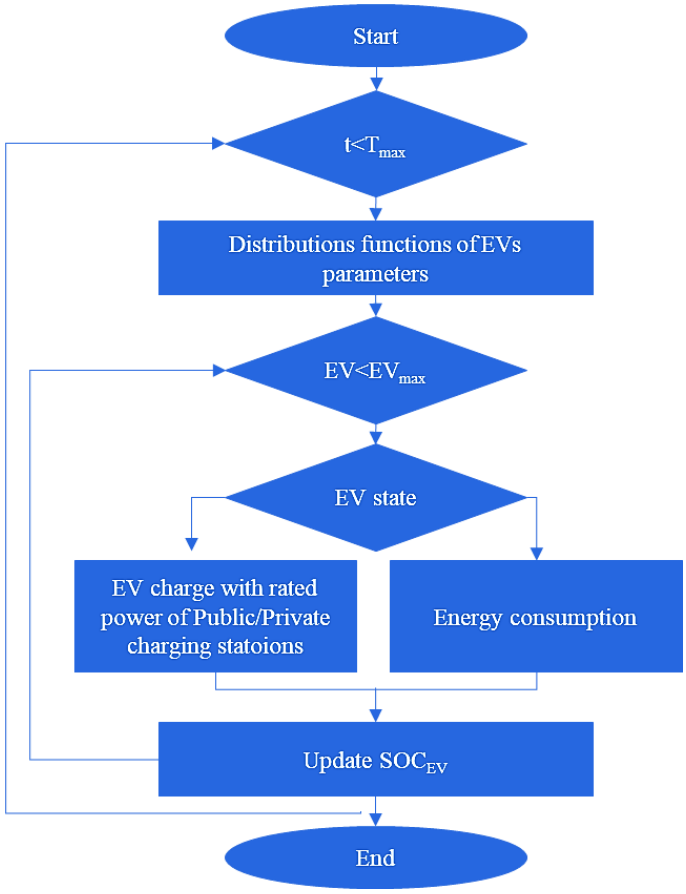

Figure 2.3 Method for EV behaviors

2.1.3 Model for the occupancy time for public electric vehicle charging station

The critical deciding factor for the number of public EVCS will be the number of EVs arriving at the charging station immediately and how many of them can wait. A detailed model has been developed for charging stations based on occupancy time. The number of EVCS depends on several parameters, such as location, usage, and budget, among others. The current study highlights the use of EVCS as the most crucial parameter. The usage of EVCS is highlighted in terms of the period when the EV occupies the EVCS. The occupancy time is defined as when EVs are already connected to EVCS, and another EV expects a time slot. The novelty of the proposed model is the relationship between the number of charging stations and the occupancy time. The concept of occupancy for EVCS is presented in figure 2.4.

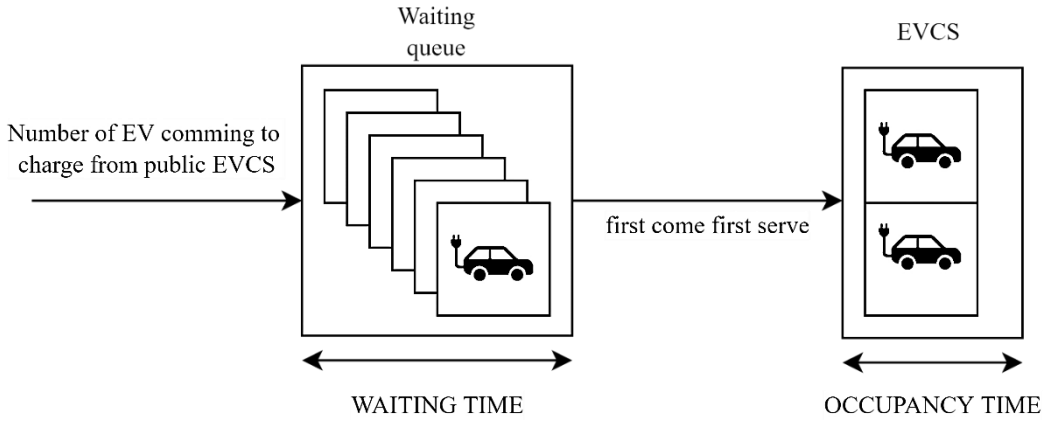

Figure 2.4 concept of occupancy time model for EVCS

Each EV in the waiting queue has an associated charging time computed in section 2.1.2. The EVs are charged from the rated power of EVCS, but the duration of charging every EV will be different as some EVs that lose more energy during traveling will charge longer. If there is only one EVCS, and the number of EVs is high, there will be queues of EVs waiting. Otherwise, the EVCS will be overestimated. Hence, the optimal number is needed for a low investment cost and a good occupancy time. A single EVCS handles two EVs simultaneously, so the third EV must wait. This waiting time of EV will determine the occupancy time of the EVCS. However, the occupancy time becomes zero during this period as no EV is waiting. Finally, the total times when the EVCS is occupied are averaged per day, and the number of EVCS is determined based on the occupancy time. A detailed description of the model to determine the number of EVCS is given in the annex.

2.1.4 Placement algorithm for public EVCS with monte-carlo simulation

The next point is to optimally place the public charging infrastructure in the electrical network so it can be supplied in the best possible way. The EVCS should be consistent and ready to power the EV with its rated power at all times without reaching the critical grid voltage. For that reason, the microgrid electrical power system without any infeed of the distributed energy resources (DERs) is considered. This is a worst-case consideration to ensure that the critical under voltage is avoided after placement. A potentially less conservative approach for the placement of EVCS is game theory through optimization [47]. However, the holistic method proposed in this paper emphasizes grid voltage stability. The optimization approach with power flow equations due to non-convexity is avoided in e-mobility infrastructure planning. This section aims to find the best nodes for EVCS placement based on the voltage stability of the microgrid before optimal planning and operation methods to avoid high complexity and intractability.

The sensitivity of the voltage to EVCS load is computed with the node voltage-sensitive index (NVSI) by using newton raphson power flow. A single EVCS station with a rated power of 22 kW is placed on the i^{th} node of the grid. In the next step, the voltages for all nodes of the grid are calculated to find the NVSI of this node i. The procedure has been repeated for every grid node. All grid nodes have the associated load computed as an input parameter in electrical load modeling depicted in figure 2.1. The grid structure and methodology for input parameters are described in [44]. The NSVI has been used for optimal distributed generation (DG) placement and load-shedding algorithms in literature [48,49]. The calculation of NVSI for a node number (i) due to the EVCS placement is stated in (2.4).

$$NVSI_i = \sqrt{\frac{\sum_{j=1}^{n}(U_{\mathrm{k}} - U_{\mathrm{j}})^2}{n}} \qquad \forall i \in j \ \ \forall j \in n \qquad (2.4)$$

Here, U_{j} is the voltage at the j^{th} node, and n is the number of total nodes. U_{k} is the nominal voltage and n is the total number of nodes. The goal is to place the EVCS in the least sensitive nodes. Due to this, the node with the highest NVSI is the worst, and the node with the least NVSI is the best node for the EVCS connection. The appropriate location for the EVCS is calculated after the best and worst nodes are found using NVSI. If there is just one EVCS, the node with the lowest NVSI is the optimal spot to deploy the EVCS. For two or more EVCS, however, the optimal node configuration must be determined. This is because installing EVCS on some nodes, even those with low sensitivity might result in a significant voltage drop across the string. The following are the reasons behind this:

- The EVCS-associated nodes may belong to the exact string.
- The EVCS is deployed on a node that can only support the installation of EVCS in a certain configuration with other nodes.

The configuration is defined as the arrangement of the number of EVCS over the available nodes. The monte-carlo simulation is deployed to identify the best configurations, as shown in figure 2.5.

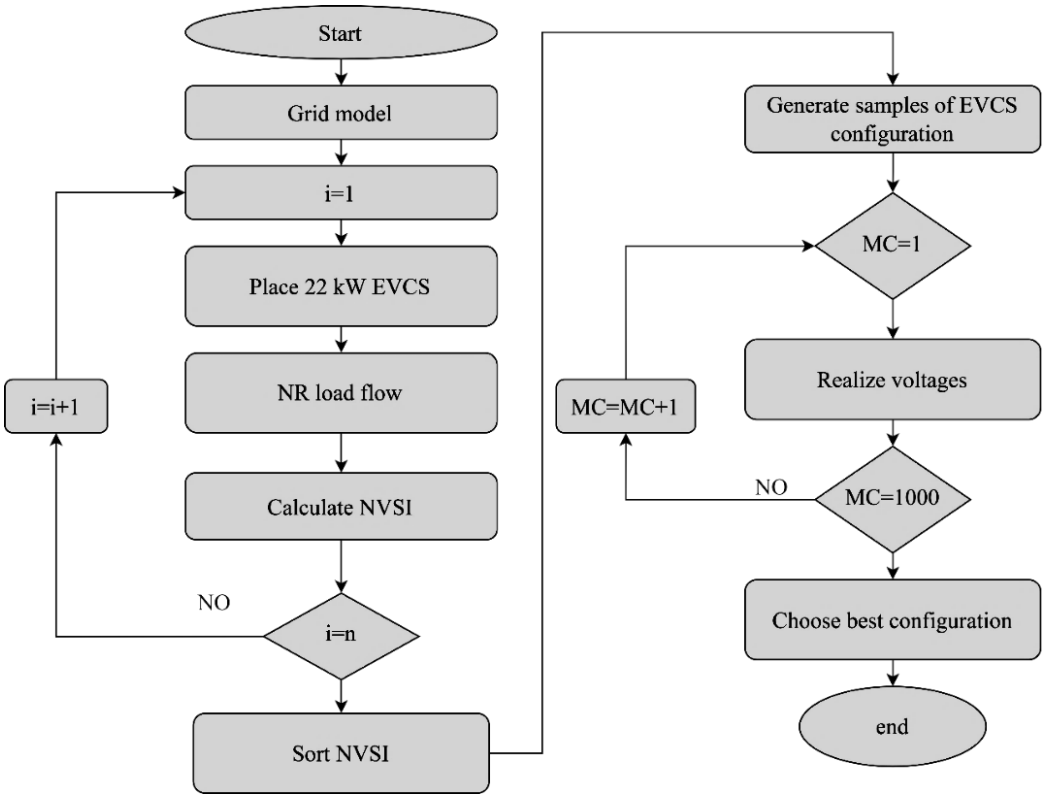

Figure 2.5 EVCS placement algorithm

First of all, the best nodes based on the sorted NVSI are taken. Then samples of configuration for the best nodes are generated for the number of EVCS known from section 2.1.3. The possible configuration samples will equal the number of monte-carlo simulation runs. For each configuration, the voltage is recorded. The configuration sample resulted in the best possible voltage being treated as optimal. The configuration which gives a voltage below 380 V at any node is discarded. The best configuration of nodes for EVCS is decided based on the

quantification of voltages. The EV load behavior described in section 2.1.2 is used as input to depict the EVCS load. The more monte-carlo iteration searches, the more configuration are analyzed on the cost of higher computational time. For an EVCS placement, the installation of EVCS is subject to available places, e.g., parking places, and the use case, e.g., near markets or public transport. Due to this, there should be a variety of configuration results. Decision-makers will then use these methods to know the suitable area and the electrical power nodes to power the EVCS. In the present study, the placement of EVCS is proposed in the ten best configurations, and the first configuration is used to place the EVCS.

2.2 Optimization methodology

The deterministic optimization is expected to be more cost-effective but cannot realize these uncertainties resulting in an un-robust or semi-robust microgrid. Due to this, stochastic microgrid planning and operation are proposed for the decision-makers, where the aim is a robust settlement area. The robustness will increase the cost of handling more uncertainties which is not a good solution. Due to this, the combined optimization model is proposed to get high robustness with minimum cost for planning a new settlement area. Microgrid planning and optimization are based on a novel concept for the growth of e-mobility infrastructure, which is performed with a planning horizon (Y) of 10 years and an operation horizon of 1 year. A 1-hour time step is used. It is assumed that the capital and operational cost will not change in the planning horizon. Furthermore, it is assumed that the electrical and heating grid structure will not be changed for the planning horizon. For optimal planning and operation, the cost parameter of the DERs used in the present study is given in table 2.2.

Table 2.2 Cost parameter of DERs per year

DERs	Terms	Values
PV	Capital cost	800 €/kW [50]
	life	20 years [51]
Wind	Capital cost	1460 €/kW [50]
	life	20 years [52]
BESS	Capital cost	528 €/kWh [53]
	life	8 years [53]
	Efficiency	95 % [54]
TESS	Capital cost	200 €/kWh [55]
	life	20 years [56]
	Efficiency	65% [57]
HESS	Capital cost	150 €/m3 [58]
	life	10 years [57]
HP	Capital cost	700 €/kW [59]
	life	20 years [60]
Fuel cell	Capital cost	5738 €/kW [61]
	life	60000 hours [62]
	Efficiency	60 % [63]
Electrolyzer	Capital cost	238 €/kW [64]
	life	60000 hours [64]
	Efficiency	70 % [63]
EVCS	Capital cost	10000 €/EVCS [65]
	life	10 years [66]

The maintenance cost is assumed to be 1 percent of the capital cost [67]. The German government plans to increase the cost of CO_2 [68]. The trend for the cost of CO_2 per ton is given in figure 2.6. In the present study, it is assumed that the CO_2 price will increase by 5 € per ton per year throughout the planning horizon in accordance with figure 2.6. The CO_2 is supposed to be emitted from the conventional generation in the connected electricity grid. The CO_2 emissions are expected to decrease yearly, as shown in figure 2.7. The average decrease in GHG was recorded as 4 percent per year from 1990 till 2021. Due to this, in the present study, it is assumed that this trend will continue to form the whole planning horizon. The penalty cost related to CO_2 emission for the microgrid is associated with all DERs especially CO_2 emitted during the manufacturing process. Moreover, the highest share is associated with the electricity grid. Due to this, the CO_2 emission associated with the manufacturing process of DERs is ignored in the present study.

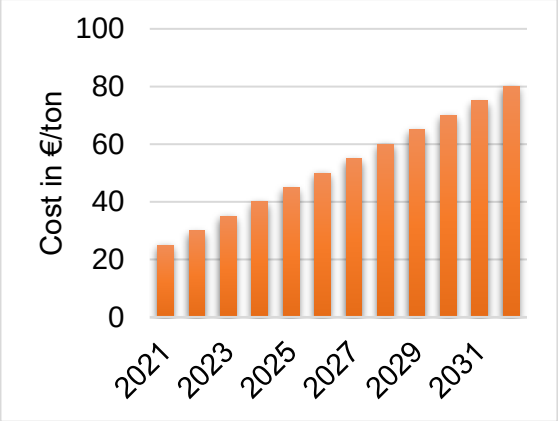

Figure 2.6 Trend for the cost of CO_2 per ton [68]

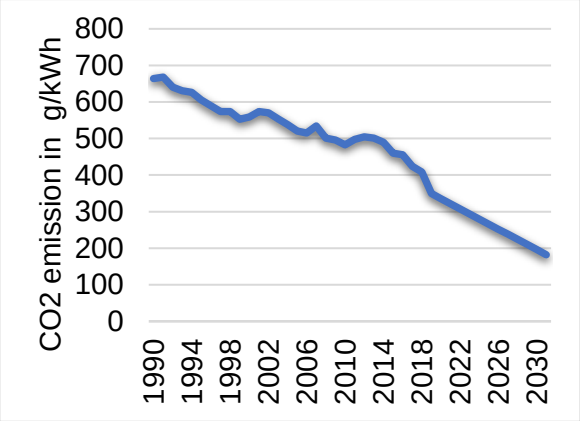

Figure 2.7 GHG emission by electricity grid [69]

2.2.1 Deterministic optimization method

The objective of the deterministic model is to decrease the investment cost C_{inv}, operational cost C_{op} and the penalty cost per ton of CO_2 emissions $C_{\text{penalty, CO2}}$ for the microgrid as given in (2.5).

$$Min \sum_{y} \left(C_{\text{inv}} + C_{\text{op}} + C_{\text{penalty, CO2}}\right) \qquad \forall y \in Y \qquad (2.5)$$

$$C_{\text{inv}} = C_{\text{PV}}\, P_{\text{PV, cap}} + C_{\text{w}}\, P_{\text{wind,cap}} + C_{\text{EESS}}\, E_{\text{EESS, cap}} + C_{\text{HP}}\, P_{\text{HP,cap}} + C_{\text{TESS}}\, E_{\text{TESS,cap}} + C_{\text{FC}}\, P_{\text{FC,cap}} + C_{\text{elec}}\, P_{\text{elec,cap}} + C_{\text{H}}\, E_{\text{HESS,cap}} \qquad (2.6)$$

$$C_{\text{op}} = \sum_{DERs} C_{\text{op, DERs}}\, P_{\text{DERs}} + \sum_{t} \left(C_{\text{grid}} P_{\text{grid}}\right) \qquad \forall t \in T \qquad (2.7)$$

$$DERs \in [PV, WIND, EESS, HP, TESS, FC, ELEC, HESS]$$

$$C_{\text{penalty, CO2}} = C_{\text{EM}} \left(EM_{\text{grid}} \sum_{t} P_{\text{grid}}\right) \qquad \forall t \in T \qquad (2.8)$$

C_{grid} is the energy import cost from the electrical grid in €/kWh. The emission intensity parameter for the electricity grid (EM_{grid}) is assumed from figure 2.7. C_{EM} is the cost of CO_2 emission and determined by figure 2.6. Based on the occupancy time, the number of EVCS is known from section 2.1, and the number of EVCS is incorporated in the energy balance constraint in the deterministic optimization model. For a fixed occupancy time, the capital cost

of the already-known number EVCS is added to the final cost of the microgrid after the optimization is solved. The optimization is subject to the following constraints,

$$P_{\mathrm{PV}}(t) + P_{\mathrm{w}}(t) + P_{\mathrm{grid}}(t) + P_{\mathrm{BD}}(t) + P_{\mathrm{FC}}(t) - P_{\mathrm{Load}}(t) - P_{\mathrm{BC}}(t) - P_{\mathrm{elec}}(t) - P_{\mathrm{HP,in}}(t) - P_{\mathrm{EVCS}}(t) = 0 \quad \forall t \in T \tag{2.9}$$

$$0 \le E_{\mathrm{ES}}(t) \le E_{\mathrm{ES,cap}} \quad , \quad 0 \le E_{\mathrm{ES,cap}} \le E_{\mathrm{ES,max}} \tag{2.10}$$

$$0 \le P_{\mathrm{DERs}}(t) \le P_{\mathrm{DERs,cap}} \quad , \quad 0 \le P_{\mathrm{DERs,cap}} \le P_{\mathrm{DERs,max}} \tag{2.11}$$

$$0 \le \gamma_1 P_{\mathrm{ES,ch}}(t) \le P_{\mathrm{ES,cap}} \quad , \quad 0 \le \gamma_2 P_{\mathrm{ES,disch}}(t) \le P_{\mathrm{ES,cap}}, \gamma_1 + \gamma_2 \le 1 \tag{2.12}$$

$$E_{\mathrm{ES}}(t+1) = E_{\mathrm{ES}}(t) + \eta_{\mathrm{ES}} P_{\mathrm{ES,ch}}(t) - \frac{P_{\mathrm{ES,disch}}(t)}{\eta_{\mathrm{ES}}} \tag{2.13}$$

$$SOC_{\mathrm{ES}}(t) = \frac{E_{\mathrm{ES}}\,(t)}{E_{\mathrm{ES,cap}}}, ES \in [EESS, TESS, HESS] \tag{2.14}$$

$$Q_{\mathrm{HP,out}} = SCOP_{\mathrm{HP}} P_{\mathrm{HP,in}} \tag{2.15}$$

$$0 \le P_{\mathrm{w}}(t) \le P_{\mathrm{w,n}}(t) P_{\mathrm{wind,cap}} \ , \quad 0 \le P_{\mathrm{PV}}(t) \le P_{\mathrm{Irr}}(t) P_{\mathrm{PV,cap}} \tag{2.16}$$

$$H_{2,\mathrm{out}} = \frac{P_{\mathrm{elec}}}{H_{\mathrm{low}}} \eta_{\mathrm{elec}} \, , P_{\mathrm{FC}} = H_{\mathrm{low}}\, H_{2,\mathrm{FC}}\, \eta_{\mathrm{FC}} \, , \, Q_{\mathrm{FC}} = P_{\mathrm{FC}} \left(\frac{1 - \eta_{\mathrm{FC}} - \Theta_{\mathrm{FC}}}{\eta_{\mathrm{FC}}} \right) \tag{2.17}$$

$$H_{2,\mathrm{HC}} + H_{2,\mathrm{FC}} - H_{2,\mathrm{out}} = 0 \tag{2.18}$$

The power production from the wind energy system is highly dependent on the wind speed v in m/s. Due to this, proximity must be considered in the process of input data selection. The capacity constraint for wind generation is given in (2.16). The constraint ensures that production is only available if the wind blows. The active power output of the turbine P_{w} is calculated based on the wind speed recorded data of DWD [70]. P_{w} is calculated as given in (2.19) and then normalized by min-max normalization, which is the most frequent approach for data normalization [71]. The smallest value of the characteristics is turned into a zero, while the highest value is turned into a one using this procedure. The normalized wind power is given in (2.19) [71].

$$P_{\mathrm{w,n}}(t) = 0.5 \rho_{\mathrm{w}} A_{\mathrm{w}} C_{\mathrm{p}} (v(t))^3 \tag{2.19}$$

Here ρ_{w} is the density of the air in kg/m^3, C_{p} is the betz value, and A_{w} is the rotor area. The capacity limit constraints related to the wind generation model are given by (2.16). The rated PV production is calculated based on pre-establish methods in (2.20) [72]. The PV generation in a time step must not be greater than the allowed limit and respect the irradiance profile. The total PV area for the areas is given by (2.21) [72].

$$P_{\mathrm{PV,max}} = G \eta_{\mathrm{M}} P_{\mathrm{R}} A_{\mathrm{PV}} \tag{2.20}$$

$$A_{\mathrm{PV}} = A_{\mathrm{R}}\, GCR \tag{2.21}$$

Where G represents the horizontal irradiance in W/m^2, η_{M} refers to the solar module efficiency, P_{R} shows the complete system performance ratio and A_{PV} is the total PV area. Solar irradiance depends on the solar modules' location, azimuth, and inclination. A_{R} is the total roof area. GCR is the ground coverage ratio, and it is assumed as 75 percent.

Power flow equations determine the voltage, power losses, and other technical aspects. However, the ordinary power flow equation consists of trigonometric functions. Due to this, these equations are non-convex and cannot be integrated into the optimization problem for

optimal global solutions. However, different methods exist to convexify power flow equations, such as semidefinite programming (SDP) and second-order cone programming (SOCP) [73]. M. E. Baran and F. F proposed the DistFlow model for radial networks and their linearization. The DistFlow model is significantly more numerically stable than the bus injection model, and its linearization provides simple analytical solutions. The branch flow is given (2.22).

$$P_{\mathrm{in}} = \boldsymbol{A}(P_{\mathrm{s}}) - \boldsymbol{A}(I_{\mathrm{n}}R_{\mathrm{n}}) + \boldsymbol{B}(P_{\mathrm{s}}),\ Q_{\mathrm{in}} = \boldsymbol{A}(Q_{\mathrm{s}}) - \boldsymbol{A}(I_{\mathrm{n}}X_{\mathrm{n}}) + \boldsymbol{B}(Q_{\mathrm{s}}) \tag{2.22}$$

Here R_{n}, X_{n}, I_{n} are the resistance, reactance, and current of the branch, respectively. The power injected P_{in} at a node must be equal to the transfer to other nodes through branches P_{s}. The incident matrix $\boldsymbol{A}$ is the connecting matrix that contains the information of the branch connection going away from the node, while $\boldsymbol{B}$ is the connecting matrix containing the information of the branch coming into the node. The introduction of squared node voltage U_{n} and current I magnitudes and relaxed DistFlow are given by [74,75].

$$v_{\mathrm{n}} = |U_{\mathrm{n}}|^2 \qquad l_{\mathrm{n}} = |I_{\mathrm{n}}|^2 \tag{2.23}$$

$$v_{\mathrm{n+1}} = v_{\mathrm{n}} - 2(R_{\mathrm{n}}P_{\mathrm{s}} + X_{\mathrm{n}}Q_{\mathrm{s}}) + (R_{\mathrm{n}}^2 + X_{\mathrm{n}}^2)l_{\mathrm{n}} \tag{2.24}$$

A second-order cone programming (SOCP) approach is taken for this study to transform into convex, given as [72,75,76].

$$l_{\mathrm{n}} \le l_{\max}\ ,\ \ P_{\mathrm{s,\,min}} \le P_{\mathrm{s}} \le P_{\mathrm{s,\,max}}\ , Q_{\mathrm{s,\,min}} \le Q_{\mathrm{s}} \le Q_{\mathrm{s,\,max}} \qquad v_{\min} \le v_{\mathrm{n}} \le v_{\max} \tag{2.25}$$

$$l_{\mathrm{n}} = \frac{P_{\mathrm{S}}^2 + Q_{\mathrm{S}}^2}{v_{\mathrm{n}}} \quad , \quad \left\| \begin{matrix} 2P_{\mathrm{S}} \\ 2Q_{\mathrm{S}} \\ l_{\mathrm{n}} - v_{\mathrm{n}} \end{matrix} \right\|_2 \le l_{\mathrm{n}} + v_{\mathrm{n}} \tag{2.26}$$

2.2.2 Long-term uncertainty modeling using the information gap decision method (IGDM)

The IGDM is a non-probabilistic decision theory for sorting alternatives and making decisions and judgments in the face of extreme uncertainties [76]. EVCS plays an important role in the microgrid planning an operation. The number of EVCS is still low. However, the rise in the EVCS is inevitable. In the current study, it is assumed that the number of EVCS is subjected to high uncertainty. If the uncertainty is considered too high, it will be assumed that no historical data, such as a probability distribution function, is available to generate an uncertainty set. The only available data is the forecasted number of EVCS. There is an information gap since there is a lack of historical beginning data to generate the uncertainty set for the growth in the EVCS. A limitation approach known as a bound method is necessary to determine the uncertainty region of information gaps uncertainty sets. In the current study, the envelope-bound method has been used to create the uncertainty set for the number of EVCS as modeled for the declining cost of the energy storage system described in [35,77]. Unlike robust optimization, the uncertainty set has one unknown variable, the uncertainty region or, more accurately, the radius of the uncertainty zone. The radius of the uncertainty region for the number of EVCS is called α_{EVCS} in the present study. The α_{EVCS} will show the gap between the predicted number of EVCS (N_{EVCS}) and the uncertain number of EVCS ($\widehat{N}_{\mathrm{EVCS}}$). The radius of the uncertainty region needs to decrease or increase depending on the problem types (risk seeker or risk-averse). The decision-makers in this study are supposed to prioritize the safe and secure planning and operation of microgrids over maximizing paybacks. As a result, the notion is referred to as the risk-averse approach, and it should be expressed as the maximum of the

uncertainty region (α_{EVCS}). The envelope-bound formulation to create the uncertainty set for the number of EVCS is given in (2.27).

$$\Gamma(\alpha_{\mathrm{EVCS}}, N_{\mathrm{EVCS}}) = \{\widehat{N}_{\mathrm{EVCS}} : |\frac{\widehat{N}_{\mathrm{EVCS}} - N_{\mathrm{EVCS}}}{N_{\mathrm{EVCS}}}| \leq \alpha_{\mathrm{EVCS}} \qquad \forall N_{\mathrm{EVCS}} \in \Gamma(\alpha_{\mathrm{EVCS}}, N_{\mathrm{EVCS}}) \tag{2.27}$$

Here Γ shows the uncertainty set and $\widehat{N}_{\mathrm{EVCS}}$ is the uncertain variable that shows the rising trend of the EVCS in the planning years. To define the region of uncertainty for the number of EVCS, α_{EVCS} is bounded as given in (2.28).

$$0 \leq \alpha_{\mathrm{EVCS}} \leq 1 \tag{2.28}$$

A zero-uncertainty region ($\alpha_{\mathrm{EVCS}} = 0$) means that there is no uncertainty, and the predicted number of EVCS is equal to the actual number of EVCS. While full-uncertainty region ($\alpha_{\mathrm{EVCS}} = 1$) means that there is severe uncertainty, and the predicted number of EVCS is equal to the upper bound of the uncertainty region. The upper and lower bounds of the uncertainty region are bounded by an envelope, as shown in (2.29) [35]. All of the uncertainty associated with the number of EVCS is considered to have happened exclusively inside this region of the envelope.

$$(1 - \alpha_{\mathrm{EVCS}})N_{\mathrm{EVCS},} \leq \widehat{N}_{\mathrm{EVCS},} \leq (1 + \alpha_{\mathrm{EVCS}})N_{\mathrm{EVCS}} \tag{2.29}$$

When considering the uncertainty associated with the number of EVCS, the objective function for IGDM-based microgrid planning and operation is regarded as a risk-averse strategy and provided by (2.30).

$$Max\ \alpha_{\mathrm{EVCS}} \tag{2.30}$$

The constraints of the optimization model are subject to component constraints given in section 2. The uncertainty region can be increased to any level as it is directly related to the number of EVCS installations. However, this resulted in high costs, which is not optimal. Finally, the robust region needs to be maximized while the cost needs to be minimized, which results in the two-level optimization problem. However, the cost objective can be transformed into a cost budget constraint which should be less than the allowed budget f_b of the microgrid as given in (2.31), (2.32), and (2.33).

$$\sum_{y} (\hat{C}_{\mathrm{inv,y}} + C_{\mathrm{op,y}} + C_{\mathrm{penalty,\ CO_2}}) \leq f_b \tag{2.31}$$

$$\begin{aligned} \hat{C}_{\mathrm{inv}} = {} & C_{\mathrm{PV}}\, P_{\mathrm{PV,cap}} + C_{\mathrm{W}}\, P_{\mathrm{wind,cap}} + C_{\mathrm{EESS}}\, E_{\mathrm{EESS,\ cap}} + C_{\mathrm{HP}}\, P_{\mathrm{HP,cap}} + C_{\mathrm{TESS}}\, E_{\mathrm{TESS,cap}} \\ & + C_{\mathrm{FC}}\, P_{\mathrm{FC,cap}} + C_{\mathrm{elec}}\, P_{\mathrm{elec,cap}} + C_{\mathrm{H}}\, E_{\mathrm{HESS,cap}} \\ & + C_{\mathrm{EVCS}}(1 + \alpha_{\mathrm{EVCS}})\, N_{\mathrm{EVCS}} \end{aligned} \tag{2.32}$$

$$\begin{aligned} \hat{C}_{\mathrm{inv}} = {} & C_{\mathrm{PV}}\, P_{\mathrm{PV,\ cap}} + C_{\mathrm{W}}\, P_{\mathrm{wind,cap}} + C_{\mathrm{EESS}}\, E_{\mathrm{EESS,\ cap}} + C_{\mathrm{HP}}\, P_{\mathrm{HP,cap}} + C_{\mathrm{TESS}}\, E_{\mathrm{TESS,cap}} \\ & + C_{\mathrm{FC}}\, P_{\mathrm{FC,cap}} + C_{\mathrm{elec}}\, P_{\mathrm{elec,cap}} + C_{\mathrm{EVCS}} N_{\mathrm{EVCS}} + C_{\mathrm{EVCS}} \alpha_{\mathrm{EVCS}} N_{\mathrm{EVCS}} \end{aligned} \tag{2.33}$$

$\hat{C}_{\mathrm{inv}}$ is the investment cost after the consideration of uncertainty. The allowable budget is associated with the microgrid's deterministic cost, which is the objective function of the deterministic optimization model, as described in section 2.2.1. The allowable budget can also be tuned as per the requirement of the decision-makers. The minimum allowable budget is equal to the deterministic cost of the microgrid, while 100 percent is equal to two times the deterministic cost of the microgrid. In the stochastic optimization model, the number of

EVCS is decided by the optimization according to the involved uncertainties. Due to this, from equation (2.33), the term $\alpha_{\mathrm{EVCS}} N_{\mathrm{EVCS}}$ are decision variables, due to which the optimization program becomes bilinear, resulting in mixed-integer non-linear programming with concave type problem. The bilinear terms have been linearized by the McCormick method [35,78]. The linearization of bilinear terms is linearized in the way described in [35].

3 Results and discussion

3.1 Case study

The proposed microgrid planning and operation strategy for e-mobility considering multi-type uncertainties has been applied to a settlement area planned in Magdeburg, Germany [79]. In the present study, the settlement is assumed to consist of twenty-five single-family houses (SFH) and six multi-family houses (MFH), with commercial real estate (CRE). From the person distribution, the settlement area consists of 249 persons. It is assumed that the settlement area is planned to be a grid-connected microgrid through a common coupling point (PCC) node. Microgrids may also be operated from a single node when linked to the local distribution network or transmission system [80].

3.2 E-mobility infrastructure

3.2.1 Development of electric vehicles

According to the "Mobilität in Deutschland" survey, the average number of cars in houses with one person, two persons, three persons, four persons, and five persons are 0.7, 1.3, 1.7, 1.8, and 1.9, respectively [81]. According to this study, there will be 133 conventional vehicles present in the settlement area. It is assumed that all vehicles will be combustion engine-based vehicles in the settlement in 2021. According to the KBA (Germany's federal motor vehicle authority), Germany's total number of registered cars is 47,715,977, with 2,917,678 newly registered vehicles in 2020, including 394,632 electric vehicles [82]. The percentage of newly registered vehicles in total registered cars held by individuals was recorded as from 6.1 to percent 7.4 percent in the last ten years [83,84]. Consequently, the percentage of newly registered vehicles in total registered cars held by individuals is 6.1 percent, with EVs accounting for 13.53 percent of newly registered vehicles. Applying this methodology to the settlement area under study, in 2022, the number of newly registered vehicles in 2020 is expected to be 8, while the number of electric vehicles will be one. The newly registered vehicle is then replaced annually by EVs through retropolation in the planning horizon. The number of newly registered EVs from 2021 to 2030 replacing the newly registered conventional vehicles. The number of EVs registered in the following year is added to the number of EVs present in the current year. The number of EVs in 2021 is zero. However, one EV will be registered in 2021, due to which the number of EVs in 2022 will be one. The number of EVs in the planning horizon is presented in figure 3.1. The population of the settlement area is expected to remain constant over the planning horizon. As a result, the number of conventional vehicles will remain unchanged. In the negative scenario, the share of the EV in 2031 will reach 12.4 percent at the end of the planning horizon. The yearly rise rate in the EV from 2022 to 2031 varies between 1.1 and 2 percent in the negative, 4.6 to 23.4 percent in the trend, and 7 to 59 percent in the positive. The number of EVs reaches 24 percent of conventional vehicles in the trend and 32.7 in the positive scenario in 2031. The trend scenario has been used to show the results of the proposed methods.

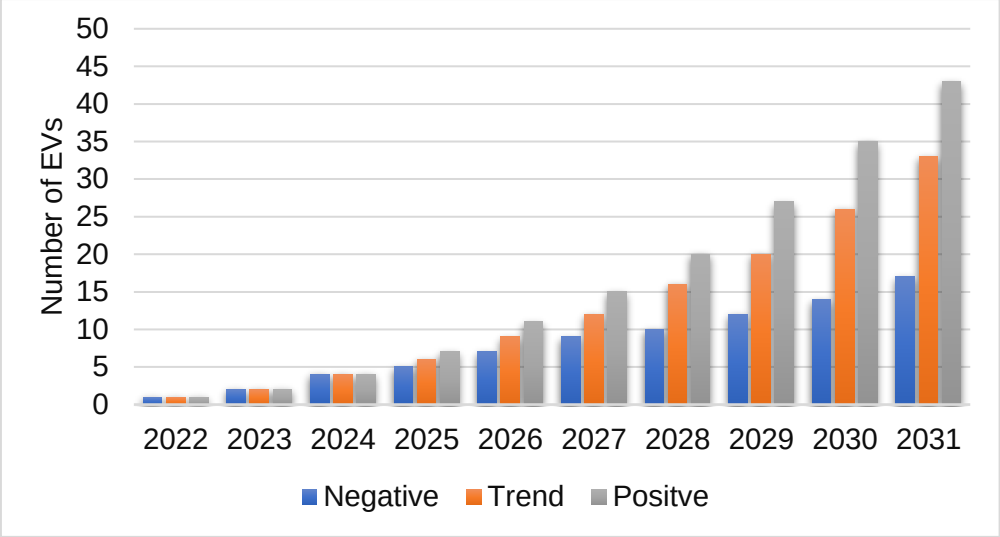

Figure 3.1 Number of newly EVs in the investigated settlement area

3.2.2 Development of private charging stations

The number of electric vehicles is essential for the settlement area as the EVs are charged in the settlement area. From an economic perspective, EVs will charge from private charging stations 85 percent of the time [45]. Once the number of EVs is known, the EV behavior is simulated as per section 2.1.2. As the settlement area is residential, the EV parameters shown in section 2.1.2 follow the residential attributes as shown in figure 3.2.

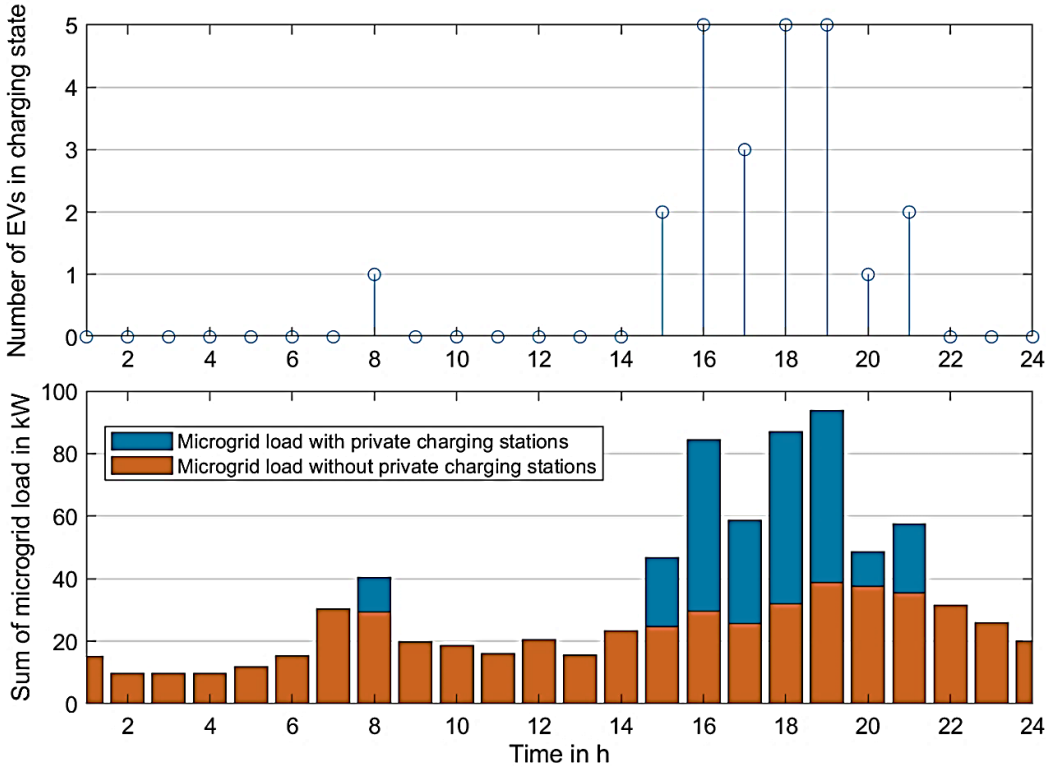

Figure 3.2 Number of EVs charging and their influence on the load of the settlement

The EV starts charging immediately after arriving with a rated power of 11 kW for a private charging station. In the trend scenario for EV development in 2031, the simultaneous arrival of EVs for charging in the settlement area and their influence on settlement load are depicted in figure 3.2 for a particular day. Note that the number of EVs in the charging state on other days

will look different due to the use of the monte-carlo simulation method. On this day, 24 EVs out of 33 needed charging from the distributed private charging stations. From 4 pm to 7 pm, the settlement area had the most significant EVs charging simultaneously, approximately 75 percent of the total EV. Due to this, the settlement area load has increased roughly 48 percent on the day. Since consumers arrive at home mostly at the same time in the evening, the EV will connect and detach nearly at the same time. The expected simultaneous charging in the settlement area for a year in the trend scenario in 2031 is shown in figure 3.3.

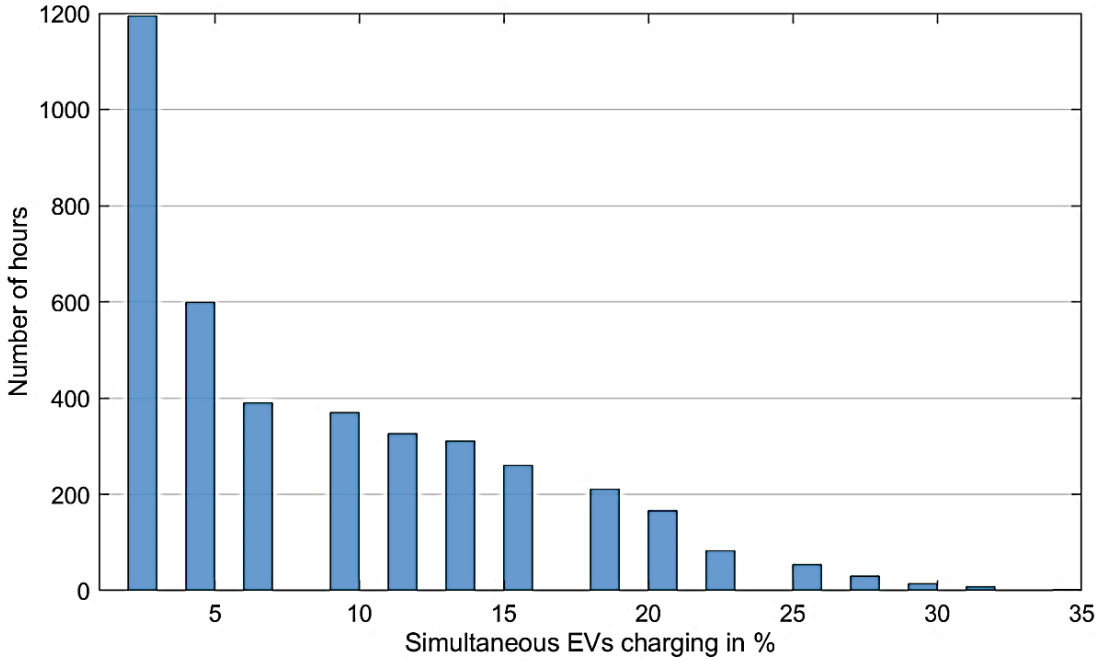

Figure 3.3 Expected percentage of EVs in simultaneous charging state in trend scenario

Most of the time years, 3 percent of EVs are charged at the same time. The largest proportion of EVs charging simultaneously is 34 percent, which occurs twice a year. The load varies in a considerably shorter time step in actuality (e.g., minutes/seconds resolution). Because EV arrivals would be more dispersed, simultaneous EV charging is expected to be significantly less in shorter time frames. The EVs coming at any moment within one hour are accumulated. The arrival of EVs is simulated at a 1-hour resolution because of a 1-hour resolution optimization hurdle. However, it is also believed that a 1-hour resolution for EV arrivals are enough for the current study, as the highest percentage of simultaneous charging rarely occurs in the year.

3.2.3 Development of public charging stations

As indicated in section 3.3, EVs will charge from public charging stations 15 percent of the time [45]. Furthermore, an EVCS often consists of two columns so that two EVs can be charged simultaneously with the rated power of the EVCS. The following statements have been planned for the public charging station in the settlement area:

- The number of EVCS based on occupancy time
- The placement for EVCS

3.2.3.1 Number of EVCS based on occupancy time

The optimal number of charging stations is determined based on the acceptable occupancy time of the EVCS, as described in section 2.1.3. The total number of EVs in the worst-case (positive scenario) rises from 1 to 43, and the occupancy time for EVs is displayed in figure 3.4.

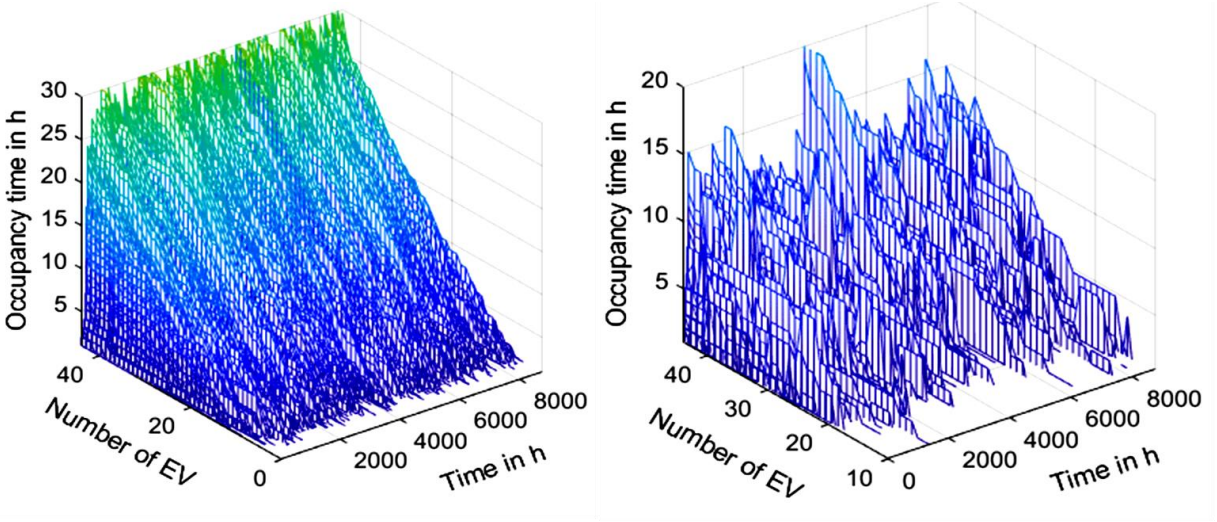

Figure 3.4 Occupancy time for EVCS=1 (left side) and EVCS=2 (right side)

When EV users arrive at a specific time, they must wait while the EVCS is used. It is clear from figure 3.3 that the likelihood of simultaneous charging is high at a particular peak for the two EVs in public EVCS. The occupancy time is calculated as the sum of all EVs waiting for a charging slot. If the number of EVs is 33 in the 2031 trend scenario and the number of EVCS is 1, the final EV will have to wait around 20 hours for a charging spot. The installation of another EVCS reduces occupancy time by roughly 50 percent for most of the year. Table 3.1 shows the occupancy time per day for increasing EVCS installation. If EVs are greater than 20, the occupancy time for the situation EVCS=1 reported in table 3.1 is much longer. The number of installed EVCS is represented as a heatmap when the total waiting time in hours for an EV is compared to the rise in the number, where high user comfort may be obtained at the cost of additional installation. If two EVCS are installed for a limited number of EVs, the occupancy time for the EV is zero.

Table 3.1 Average EVCS occupancy time per day in hours

Number of EV	**EVCS = 1**	**EVCS = 2**	**EVCS = 3**	**EVCS ≥ 4**
1-10	0	0	0	0
10-20	0-0.35	0-0.02	0	0
20-30	0.41-1.54	0.02-0.13	0	0
30-40	1.61-3.55	0.15-0.54	0-0.06	0
Over 40	3.81-6.76	0.67-1.45	0.15-0.42	0-0.039

The anticipated EVCS for the planning Horizon is indicated in table 3.2 using an EVCS occupancy duration of fewer than 30 minutes as an acceptable value.

Table 3.2 Number of EVCS for acceptance occupancy time of 30 minutes

Scenario	2022	2023	2024	2025	2026	2027	2028	2029	2030	2031
Negative	1	1	1	1	1	1	1	1	1	1
Trend	1	1	1	1	1	1	1	2	2	3
Positive	1	1	1	1	1	1	2	2	3	4

The arrival of EVs for charging is primarily influencing the occupancy time. The arrival of EVs is mainly noticed in the evening. The utilization of an EVCS by the number of EVs is an interesting parameter to be evaluated for a certain occupancy time. For an EVCS without any occupancy time, the EVs charged 15 percent of the time, as described in section 3.2. However, the utilization will change by introducing the occupancy time. The occupancy of less than 30 minutes and the utilization of the number of EVCS for the trend scenario in 2031 are shown in figure 3.5. The utilization of the EVCS will increase with the number of EVs.
Similarly, the increase in the EVs increases in the occupancy time. Due to this, the increase in the occupancy time increases the utilization of the EVCS. The utilization of the EVCS in terms of the number of hours in the year is 39.2 percent. Compared to the assumed value of 15 percent, it is concluded that the occupancy time of 30 minutes will increase the utilization by 24 percent more. Critically, the acceptability of this waiting time by the EVCS users is a barrier.

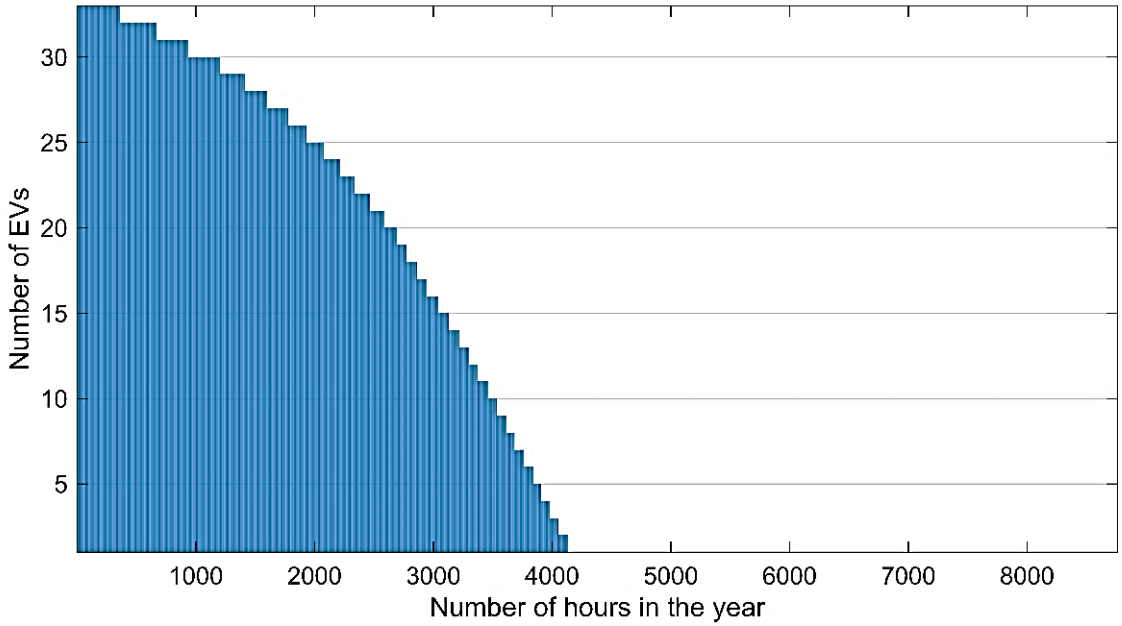

Figure 3.5 Utilization of EVCS for less than 30 minute occupancy time

However, the decision-making is based on an economic point of view as a trade-off between the lowest possible occupancy time and user acceptancy. Due to this, less occupancy time leads to less utilization which cannot be economical, and higher occupancy time leads to less acceptancy. From table 3.1 and figure 3.5, an occupancy time of less than 30 minutes seems ideal due to the economical utilization and comparable number of EVs per EVCS.

3.2.3.2 Placement of public EVCS

Typically, the best place to install a high load is near the transformers. However, this is true for a transformer with a single string. This microgrid electrical network consists of multiple strings. This leads to different influences if a new component is placed. In addition to the connection point, EVCS placement is subject to several criteria, including the available places to charge the EVs, such as park places, and suitable areas, such as proximity to markets and public transport. If the location of the EVCS place is known, the suitability of different connection nodes in other strings is investigated using the NVSI according to section 3.4. When the EVCS is put on node 1, its effect on voltage is not confined to that node but may be seen across the microgrid. As seen in equation (2.4), the NVSI examined the impact of an EVCS on all nodes

belonging to the settlement. The results for the NVSI of the various nodes are summarized in figure 3.6.

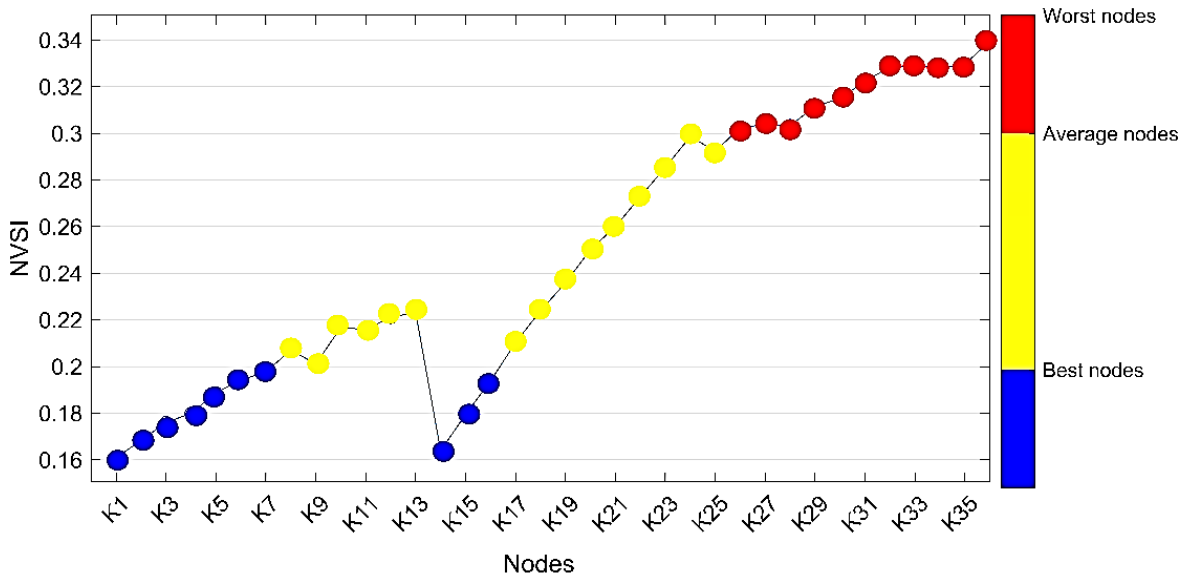

Figure 3.6 NVSI for the settlement area

The best connection point for an EVCS is the nodes with the lowest NVSI. In general, the nodes of a shorter string with fewer houses are preferable to a longer string with a more significant number of houses. However, not all nodes in the former string are insensitive to all nodes in the later string. From figure 3.6, the 2nd node of the first string shows higher NVSI than the 1st node of the second string. This concludes that the 2nd best location for an EVCS is the first node of string 2. Table 3.3 shows the ideal configuration for the trend scenario.

Table 3.3 Configuration suggestion for trend scenario in 2031

Knoten	1	2	3	4	5	6	7	8	9	10
K1	1	1	1	1	1	1	1	0	0	0
K14	1	1	0	1	0	0	0	1	1	0
K2	1	0	1	0	1	0	0	1	0	0
K3	0	0	0	1	0	1	0	0	0	1
K15	0	1	0	0	1	1	1	0	0	0
K4	0	0	1	0	0	0	0	0	0	1
K5	0	0	0	0	0	0	1	0	1	0
K16	0	0	0	0	0	0	0	1	0	0
K6	0	0	0	0	0	0	0	0	1	0
K7	0	0	0	0	0	0	0	0	0	1

Ten nodes are qualified as best prospects nodes if their NVSI is less than 0.2. Once the optimum nodes for one EVCS have been identified, the ideal configurations for several EVCS are investigated. Each column of table 3.3 represents one configuration of EVCS placement. Finally, the first configuration is chosen to place EVCS for the investigated settlement area in 2031, based on the optimum configuration from table 3.3.

3.3 Deterministic microgrid planning and operation for e-mobility

As the heat and electrical demand are defined, the microgrid consisting of DERs is optimally sized using the mixed-integer non-linear problem described in section 2.2. The optimization

results as a convex problem with mixed integer non-linear programming (MINLP) solved with the help of the gurobi solver, and the YALMIP tools box is used for formulation [85].
The planning is considered a multi-period where the capacities are decided yearly. The last year of the planning horizon can be seen as the final capacity for future planning. Any capacities for any year in this planning horizon are ideal. For instance, in a 5-year planning horizon, any capacities are optimal at the end of 5 years.

3.3.1 Microgrid DERs dimensions

The EESS and TESS capacities are measured in kWh, whereas the generating units, heat pump, and electrolyzer are measured in kW, and the HESS is measured in m^3. As seen in figure 3.7, generation sizes expand exponentially as the number of EVs increases. PV, wind, and EESS will reach their maximum capacity in 2026, and as EVs grow more prevalent, the fuel cell will rise to handle the larger load.

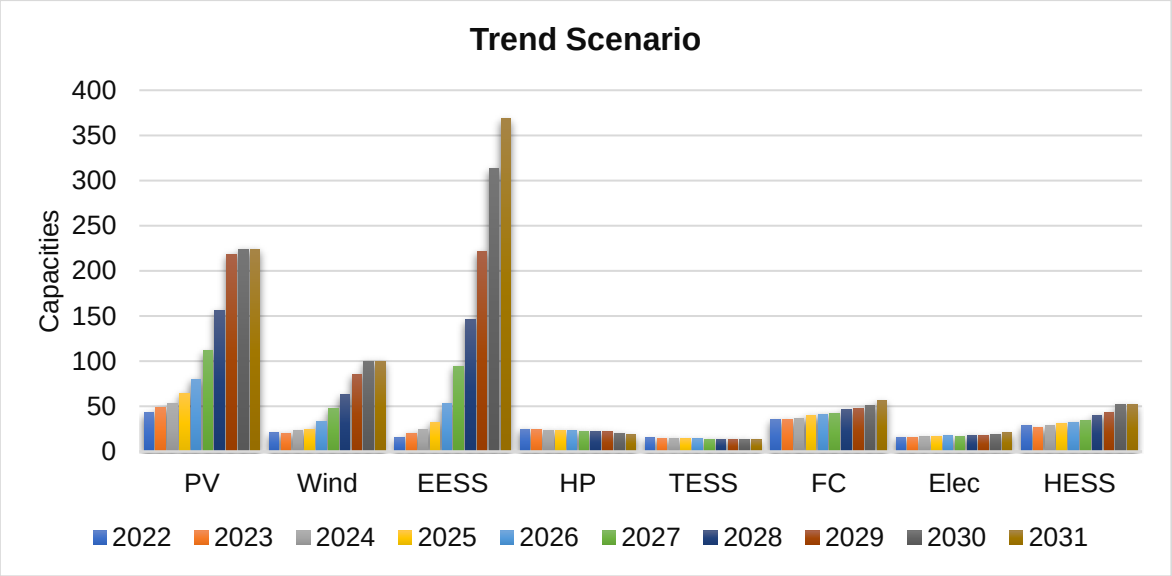

Figure 3.7 Microgrid capacity

Since the fuel cell creates heat and electricity, it has a larger capacity than the EESS. However, if the electric load grows due to the increase in EVs, the EESS gains more capacity. This is because the fuel cell is more costly, and the heat load is not changing in the planning horizon. Consequently, an increase in the electric vehicle sparked a slight increase in the fuel cell, resulting in a minor drop in the heat pump. The hydrogen storage and electrolyzer will also increase with the rise in the fuel cell. The community is situated in a residential part of the city. As a result, traditional large wind turbines are not viable to construct.
On the other hand, small wind turbines must be put in communities to meet GHG reduction requirements. Small private wind turbines will not be able to be built in the examined settlement area since the houses are equipped with PV systems. As a result, medium-sized wind turbines with low noise and fewer areas are advised. A medium-sized wind turbine with a hub height of 20 m and rated power of 15 kW is commercially available [86]. For district heating, the larger heat pumps, fuel cells, and TESS systems are available on a kW scale [87,88].

3.3.2 Microgrid cost analysis

The optimization objective of the deterministic approach defined in section 4.1 is to plan and operate with minimum cost. The settlement area's total cost includes investment, operational,

and emissions penalty costs. The total cost of the microgrid for the planning horizon for negative, trend, and positive scenarios is given in figure 3.8.

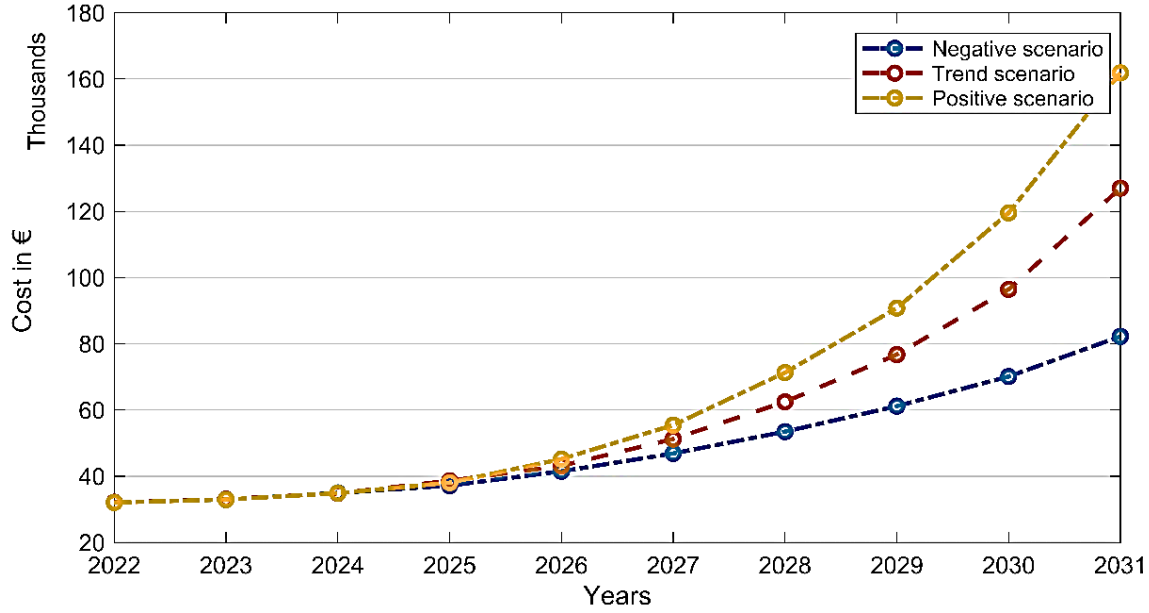

Figure 3.8 Overall cost of the settlement area for different scenarios

Due to the same number of EVs, the cost of the microgrid at the start of the planning horizon is nearly the same. As the number of electric vehicles increases toward the end of the planning horizon, the cost difference between scenarios will widen. In 2031, taking the trend scenario as a reference, this cost will be 12.6 percent lower in a negative scenario. The percentage of cost rise in 2031 for the positive scenario compared to the trend scenario is 32 percent in 2031. The increase in the settlement's overall cost per increase in the number of EVs is evaluated. It is observed that per EV will increase by 2.3 to 2.9 percent in the settlement cost. The comparison of the overall cost in terms of investment, operation, and penalty cost related to CO_2 is shown in figure 3.9. In the trend scenario, investment costs generated 58.4 percent of the total cost, operating costs contributed 38.4 percent, and CO_2 costs contributed just 3.1 percent. From figure 3.9, the costs will follow the capacities. Due to this, it can be observed that the investment cost significantly influences the capacities. The operation cost comprises the electricity imported from the connected grid and the maintenance cost of DERs, which is assumed to be 1 percent of the capital cost of DERs. The investment cost will increase at a low rate till 2026, but after that, the number of EVs will increase more rapidly, resulting in a steep increase in capacities. The EVs are still rising till 2031, which needs to be fulfilled by the grid import. The penalty cost for CO_2 emission is not increasing at a high rate because the emission cost certificate for CO_2 is rising every year. The optimization tries to minimize it as much as possible. Compared to operation cost, the CO_2 penalty cost is too low because the CO_2 emission certificate cost per tonne is still too low in Germany. For that reason, CO_2 cost is maybe not the best instrument to support local decentral DERs. The high number of EVs will increase the load, due to which the operational cost compared to CO_2 emission cost will grow at a higher rate. This may become a barrier for a microgrid investment with the motivation of less CO_2 emissions. Due to this, the emission certificate cost needed to be increased to support higher renewables integration in the communities.

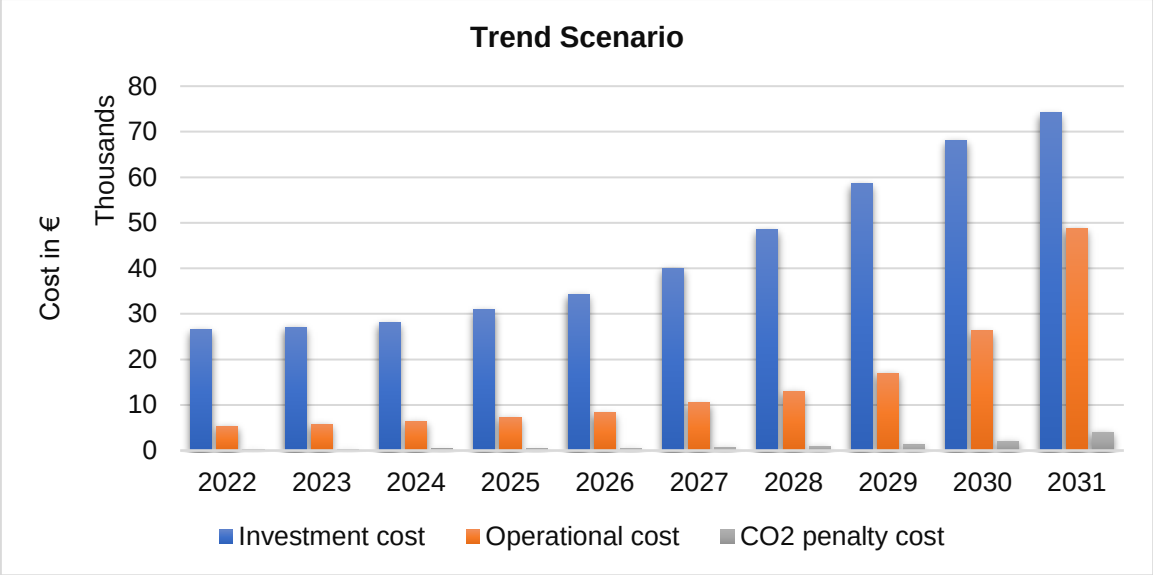

Figure 3.9 Cost analysis of microgrid

Given that the distribution grid supplies all of the microgrid's energy needs, 190.5 MWh of grid energy must be obtained in the present situation. The required energy will cost 57,150 € or around 56.2 percent more than the optimally planned microgrid represented in figure 3.8. The cost of the CO_2 emission penalty has also decreased from 857.2 € to 219.64 €, significantly reducing the carbon footprint. Similarly, for trend 2031, the cost of a microgrid without any DERs increases to 1,79,700 €, which has been reduced to 127,029 €.

3.4 Microgrid planning and operation with stochastic optimization

The increase in the EV and EVCS is inevitable, as described in section 2. The forecast is just based on the factors described in section 2. However, it is challenging to forecast these rises in the EVCS accurately because any of these factors may change. Based on the recent crises such as pandemics and shortages of semiconductor materials, EV production has been affected immensely, affecting the installation of EVCS. It is clear that the actual number of EV and EVCS installations has not been following the trends due to several reasons. This is predicted to have a significant impact on microgrid planning and operation. For the evaluation of the results, the trend scenario is considered. The microgrid is considered in a risk-averse manner (risk-avoiding). If the ability of the DERs of the microgrid to amount of uncertainties occurs defines the robustness of the microgrid. A best-case in terms of a risk-averse microgrid is when fewer uncertainties occur and vice versa. However, the uncertainties are uncontrollable, due to which the robustness of the microgrid should be planned. The envelope bound for the number of EVCS shows the boundary of the uncertainty region.

The optimization aims to increase the robust region α_{EVCS} concerning the allowed budget f_{b}. The allowed budget is defined as the percentage increase in the cost of the microgrid achieved from the deterministic optimization. f_{b} will be equal to the cost of the deterministic microgrid if the allowed budget is 1. The decision-maker can adjust this factor at the planning stage based on the amount of acceptance to pay more for the microgrid's robustness against uncertainty. The α_{EVCS} will change depending on the specified f_{b} and the highest attainable α_{EVCS} will be the ultimate microgrid robustness against EVCS uncertainty. The robustness of the microgrid with the change in the allowable budget is shown in figure 3.10. It can be seen from figure 3.10

that the uncertainty region increases linearly with an increase in the allowable cost budget. A 100 percent robust region can be achieved with an allowable budget of 1.8.

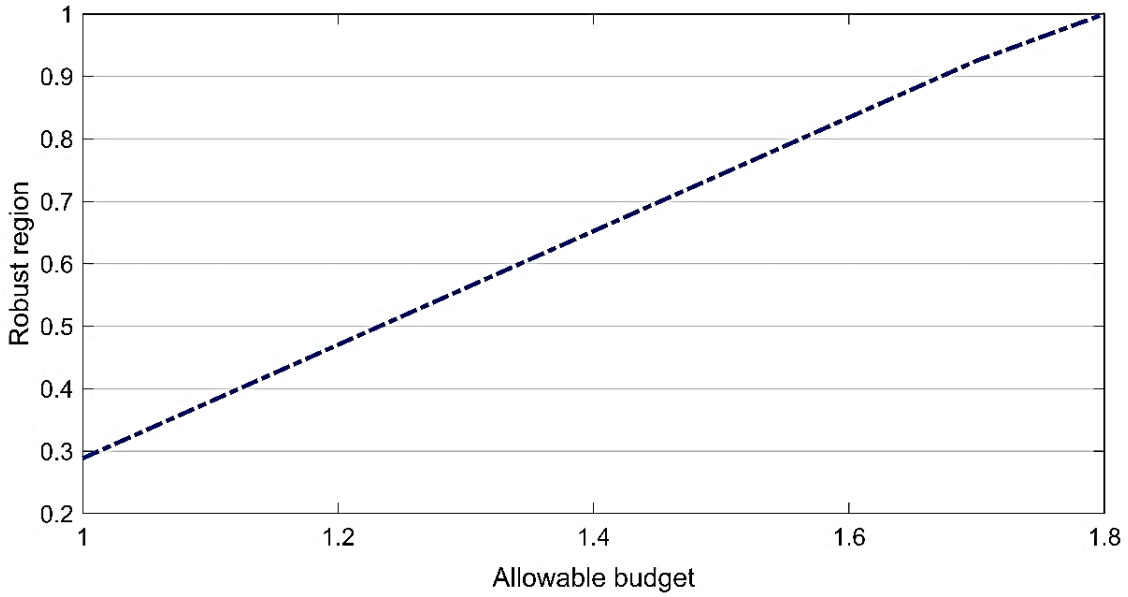

Figure 3.10 Robust region versus allowable budget

This means that 1.8 times (80 percent) more cost is needed for the microgrid to handle all uncertainties in the envelope. For an allowable budget equal to the deterministic cost, the microgrid has similar DERs capacities as computed in the deterministic optimization model. Considering the allowable budget equal to the deterministic cost, the microgrid has only 28.8 percent of robustness under long-term uncertainty. A higher budget increased the capacities of the DERs to power the extra amount of EVCS, which will increase the robustness of the microgrid. The capacities of DERs for trend scenarios for a 100 percent robust (allowable budget of 1.8) are shown in figure 3.11.

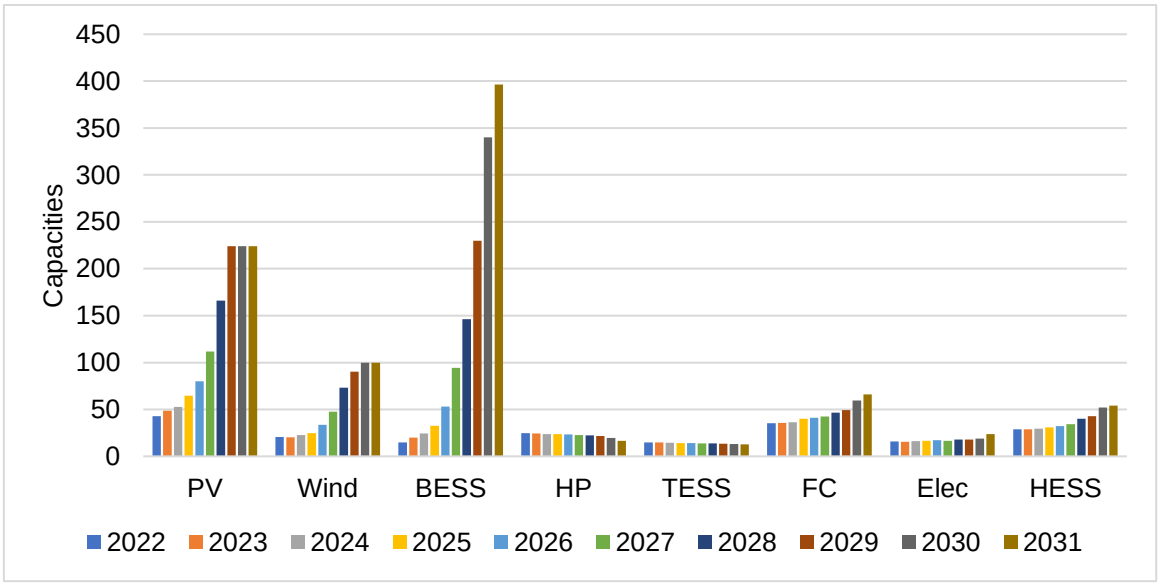

Figure 3.11 Microgrid capacities of trend scenario

Uncertainties are unavoidable, but the number of uncertainties is difficult to estimate. As a result, a fully robust microgrid is proposed at a higher cost during the planning stage. It may

be more expensive to tackle these uncertainties economically and technically if the microgrid is designed for less resilience and more uncertainty occurs. The 80 percent increase in the microgrid's cost budget to meet the additional number of EVCS enhances the capacity of the PV and EESS. This increase in PV, wind, and EESS will ensure that the EVCS is powered more by renewable energy. Most of the long-term uncertainties occur at the end of the planning horizon. In these years, the PV and wind systems cannot be increased further due to the limits for integrating into the low voltage grids. Due to this, the capacity of the EESS and fuel cell increases more as compared to the deterministic approach. As the number of EVCS rises, the number of uncertainties increases. As illustrated in figure 3.11, the capacities increase in the same fashion. The heating equipment is not frequently changed because the heating grid and heating demand are consistent. The slight drop in the heat pump is caused by an increase in the fuel cell required to generate electric power due to uncertainties in conjunction with other generation units. The proposed method based on IGDM is highly recommended over the deterministic approach when there is a chance of the occurrence of long-term uncertainty, which cannot be realized through the deterministic optimization approach. The cost of a 100 percent robust microgrid with DERs needs 80 percent more cost than a microgrid without any uncertainty. Furthermore, compared to a microgrid without any DERs, the cost is still greater by an amount of 48948.6 €, which is 37 percent. This amount must be included in the microgrid planning to avoid any problems that occur due to severe uncertainty.

4 Conclusion and outlook

In the scope of this study, a new holistic approach for microgrid planning and operation for e-mobility under consideration of multi-type uncertainties was proposed and discussed. The scope of this study was to develop a cost-efficient, emission-effective, and technically sound microgrid from scratch for the development of e-mobility infrastructure, as well as to analyze the consequences of e-mobility-related uncertainties on the microgrid.

Due to the motivation to address climate change, developing renewable energy sources, energy storage systems, and sector coupling technologies, also known as distributed energy resources, is inevitable in sectors such as electricity, heat, and industry. Similarly, the e-mobility infrastructure is developing rapidly as a result of this motivation. Renewable energy sources must power the e-mobility infrastructure to achieve environmental effectiveness over combustion engine vehicles. However, the existing power systems are not always capable of handling the additional power and adverse effects of large-scale deployment of e-mobility infrastructure.

The methods were implemented in a case study of a new settlement area Alte-ziegelei Magdeburg, Germany. The settlement area is planned from scratch, where the statistics and available areas for PV systems with settlement demand are modeled. A microgrid based on the above-stated method is planned for a planning horizon of 10 years for the investigated settlement area. Based on people's acceptance, three scenarios (negative, trend, and positive) for the development of the number of electric vehicles are generated. Based on investment costs, operational costs, driving benefits, and other benefits, a projection for the percentage of EVs over conventional cars in 2026 is made. The rising rate of EVs is then retropolated till 2026 and extrapolated till the end of the planning horizon. It was concluded that the number of EVs will be one in 2022, which will be raised to 17, 33, and 43 in negative, trend, and positive scenarios, respectively. At the end of the planned horizon, electric vehicles might constitute up to 31 percent of all vehicles. In the investigated settlement area, these EVs will be charged at home using private charging stations with a rated power of 11 kW and at public electric vehicle charging stations with a rated power of 22 kW. Based on the results for EVs behaviors from

the monte-carlo simulation, the EVs will increase the electrical load up to 48 percent on a particular day. Furthermore, because consumers arrive at their homes mostly at the same time in the evening, roughly 3 to 34 percent of all EVs might be charging simultaneously, resulting in a significant peak in the settlement load. In the trend scenario, the EV in the settlement area will require at least three EVCS by 2031, based on EVCS occupancy times of less than 30 minutes. The planned three EVCS must be installed at the nodes with a node voltage-sensitive index (NVSI) of less than 0.2. Due to this, the optimal location for the public EVCS was concluded to be K1, K14, and K2.

The investigated settlement area is optimally planned and operated using a deterministic optimization approach based on the rise in EVs. When comparing the negative, trend, and positive scenarios, the overall cost of the investigated settlement area decreased by 12.6 percent in the negative scenario and increased by 32 percent in the positive scenario. A rise per EV in the settlement area indicates a 2.3 to 2.9 percent increase in overall cost. The dimension of the DERs in the investigated settlement area for the trend scenario for 2031 is shown in table 4.1.

Table 4.1 DERs dimension in 2031 for investigated settlement area

DERs	PV	Wind	EESS	HP	TESS	FC	Elec	HESS
Capacities	224. kW	100 kW	368.3 kWh	18.6 kW	12.8 kWh	56.0 kW	20.8 kW	52.3 m^3

In the trend scenario, implementing these DERs in the settlement area needed an overall cost of 1,27,029 €. 58.4 percent of the cost is contributed by investment cost, 38.4 percent is contributed by operation cost, and only 3.1 percent is contributed by the CO_2 penalty cost. To completely protect against long-term problems in the development of EVCS, the cost of the microgrid must be increased by 80 percent. When compared to a microgrid without any DERs, a decrease of 56.2 percent is seen.

Considering the long-term uncertainties, it was concluded that the microgrid resulting from the deterministic approach is just 28 percent robust against the long-term uncertainty. Such low robustness will be risky in long-term planning. To achieve complete robustness, the cost of the microgrid needs to be increased by 80 percent. The increase in the cost resulted from the higher capacities needed to hedge the uncertainties. Due to this, the deterministic approach is considered to be better in terms of cost, and IGDM is recommended if the robustness against uncertainties needs to be planned. Additionally, a microgrid that is entirely resilient has seen costs increase by around 37 percent more as a result of severe uncertainties. Due to the robustness of the permitted budget of 80 percent, 66.7 percent of the cost has grown in comparison to the deterministic technique in the trend scenario in 2031.

References

[1] K Appunn, F Eriksen and J Wettengel, "Journalism for the energy transition," 16 August 2021. [Online]. Available: https://www.cleanenergywire.org/factsheets/germanys-greenhouse-gas-emissions-and-climate-targets. [Accessed 30 August 2021].

[2] "Greenhouse Gas Emissions from Energy: Overview," IEA, August 2021. [Online]. Available: https://www.iea.org/reports/greenhouse-gas-emissions-from-energy-overview. [Accessed 30 August 2021].

[3] Z A Styczynski and P Komarnicki, "E-Energy- Projekt RegModHarz und IKTEM-Projekt Harz.EE-Mobility: Integration von Elektromobilität in den Netzbetrieb," Innovative Informations- und Kommunikationstechnologien als Rückgrat von Smart Distribution 2011, Darmstadt, 2011.

[4] P Franz, I Talavera, I Sgoff and J Hanson , "Optimized Regulation of Dispersed Generation Units for Minimization of reactive power consumption," in Power Energy Society Innovative Smart Grid Technologies Conference (ISGT), 2015.

[5] C Li, X Jia, Y Zhou and X Li, "A microgrids energy management model based on multi-agent system using adaptive weight and chaotic search particle swarm optimization considering demand response," Journal of Cleaner Production, vol. 262, pp. 121-247, 2020.

[6] J C Alberizzi, M Rossi, and M Renzi, "A MILP algorithm for the optimal sizing of an off-grid hybrid renewable energy system in South Tyrol," in 6th International Conference on Energy and Environment Research, Portugal, 2019.

[7] W J Huang, N Zhang, J W Yang,Y Wang, and C Q Kang, "Optimal configuration planning of multi-energy systems considering distributed renewable energy," IEEE TransSmart Grid, vol. 10:1452–64, 2019.

[8] A Ehsan and Q Yang, "Scenario-based investment planning of isolated multi-energy microgrids considering electricity, heating and cooling demand," Appl Energy, vol. 235:1277–88, 2019.

[9] M Шилер and E Рублевский, "Microgrid – ответ на новые вызовы электроэнергетики," Control engineering, vol. 70, pp. 79-83, 2017.

[10] B Tan, H Chen, X Zheng and J Huang, "Two-stage robust optimization dispatch for multiple microgrids with electric vehicle loads based on a novel data-driven uncertainty set," International Journal of Electrical Power & Energy Systems, vol. 134, pp. 107-359, 2022.

[11] S A Amamra and J Marco, "Vehicle-to-grid aggregator to support power grid and reduce electric vehicle charging cost," IEEE Access, no. 7:178528–38, 2019.

[12] C Wu, S Gao, Y Liu,T E Song and H Han, "A model predictive control approach in microgrid considering multi-uncertainty of electric vehicles. Renewable energy," Renewable Energy, vol. 163, pp. 1385-1396, 2020.

[13] L Jia, Z Hu, Y Song and Z Luo, "Optimal siting and sizing of electric vehicle charging stations," in IEEE Int. Elect. Veh. Conf, Greenville.

[14] S B Payam, R G Abbas and K K Hosein, "Optimal fast-charging station placing and sizing. Applied Energy," Applied energy, vol. 125, no. 214, pp. 289-299, 2014.

[15] G Shaoyun, F Liang, L Hong and W Long, "The planning of electric vehicle charging station in urban area, Electric & Mechanical Engineering and Information Technology (EMEIT) Conference," no. 1598-1604, 2012.

[16] X Dong, Y Mu, H Jia, X Yu and P Zeng, "Heuristic Planning Method of EV Fast Charging Station on a Freeway Considering the Power Flow Constraints of the Distribution Network," Energy Procedia, pp. 2422-2428, 2017.

[17] L Pan, E Yao, Y Yang and R Zhang, "A location model for electric vehicle (EV) public charging stations based on drivers' existing activities," Sustainable Cities and Society, pp. 102-103, 2020.

[18] P Phonrattanasak and L Nopbhorn, "Optimal location of fast charging station on residential distribution grid," International Journal of Innovation and Technology, pp. 675-681, 2012.

[19] C H Dharmakeerthi, N Mithulananthan, and T K Saha, "Modelling and planning of EV fast charging station in power grid," Power and Energy Society General Meeting, IEEE, pp. 1-8, 2012.
[20] P Phonrattanasak and L Nopbhorn, "Optimal placement of EV fast charging stations considering the impact of electrical distribution and traffic condition," International Conference on and Utility Exhibition on Green Energy for Sustainable Development (ICVE), pp. 1-6, 2016.
[21] D P Rini, S M Shamsuddin and S S Yuhaniz, "Particle swarm optimization: technique, system and challenges," pp. 19-27, 2011.
[22] Z f Liu, W Zhang, X Ji and K Li, "Optimal planning of charging station for electric vehicle based on particle swarm optimization," IEEE Innovative Smart Grid Technologies-Asia, pp. 1-5, 2012.
[23] J Prasomthong, W Ongsakul, J Meyer, "Optimal placement of vehicle- to-grid charging station in distribution system using particle swarm optimization with time varying acceleration coefficient," International Conference and Utility Exhibition on Green Energy for Sustainable Development (ICUE), pp. 1-8, 2014.
[24] S Mardle and S Pascoe, "An overview of genetic algorithms for the solution of optimization process," Comput Higher Educ Econ Rev, pp. 16-20, 1999.
[25] S Ge, L Feng and H Liu, "The planning of electric vehicle charging station based on grid partition method," IEEE electrical and control engineering conference, China:, pp. 2726-30, 2011.
[26] Y Li, L Li, J Yong,Y Yao and Z li, "Layout planning of electrical vehicle charging Stations based on genetic algorithm," Lecture Notes in Electrical, p. Lecture Notes in Electrical, 2011.
[27] Z Bendiabdellah, S M Senouci and M Feham, "A hybrid algorithm for planning public charging stations," Global Information Infrastructure and Networking Symposium (GIIS), pp. 1-3, 2014.
[28] P S You and Y C Hsieh, "A hybrid heuristic approach to the problem of the location of vehicle charging stations," Computers & Industrial Engineering, pp. 195-204, 2014.
[29] L Yan, "Optimal layout and scale of charging stations for electric vehicles," in CIRED China International Conference on Electricity Distribution (CICED), Rome, 2016.
[30] X Yan, C Duan, X Chen and Z Duan, "Planning of electric vehicle charging station based on hierarchic genetic algorithm, Transportation Electrification Asia- Pacific (ITEC Asia-Pacific)," in IEEE Conference and Expo Transportation Electrification Asia-Pacific (ITEC Asia-Pacific), 2014.
[31] S Pazouki, A Mohsenzadeh and M R Haghifam, "Optimal planning of PEVs charging stations and demand response programs considering Optimal planning of PEVs charging stations and demand response programs considering," in Smart Grid Conference (SGC), 2013.
[32] Z Liu, F Wen and G Ledwich, "Optimal planning of electric-vehicle charging stations in distribution systems," IEEE Transactions on Power Delivery, vol. 28, no. 1, pp. 102-110, 2013.
[33] A Ip and S F Liu, "Optimization for allocating BEV recharging stations in urban areas by using hierarchical clustering," in International Conference on Advanced Information Management and Service, Seoul, Korea, 2010.
[34] A Y S Lam, Y W Leung and X Chu, "Electric vehicle charging station placement," in IEEE International Smart Grid Communications, Vancouver, 2013.
[35] J Wei, Y Zhang, J Wang, X Cao, and M A Khan, "Multi-period planning of multi-energy microgrid with multi-type uncertainties using chance constrained information gap decision method," Applied Energy, 2020.
[36] "Low voltage cable ratings," Kei-ind.com, [Online]. Available: [Online]. Available: http://www.kei-ind.com/images/pdf/lt-cables/4core-aluminium-pvc-armoured.pdf. [Accessed 23 June 2020].
[37] "4 Core Aluminium PVC Armoured power cables," gridcables.com, [Online]. Available: https://www.gridcables.com/pdfs/4-core-al-armd.pdf. [Accessed 23 June 2020].
[38] "BMWi," FEDERAL MINISTRY FOR ECONOMIC AFFAIRS AND CLIMATE ACTION Germany, 13 December 2021. [Online]. Available: https://www.bmwi.de/Redaktion/EN/Artikel/Energy/electricity-grids-of-the-future-01.html. [Accessed 20 December 2021].

[39] "DIN EN 50160:2011-02," Beuth publishing DIN, 02 2010. [Online]. Available: https://www.beuth.de/en/standard/din-en-50160/136886057. [Accessed 12 November 2021].
[40] VDI, Association of German Engineers, "progress report VDI - No. 560 -. Refernezlastprofile of single and multi-family dwellings for the use of CHP plants," VDI, Düsseldorf, 2007.
[41] J Brinken, T Schulz, S Helm, N Schmidt and I Hauer, "Integrated charge site allocation for electric vehicles," in European Transport Conference, Henley-in-Arden, United Kingdom, 2020.
[42] I Hauer, M Tayyab, S Helm, M Heuer, J Brinken, M Müller, N Schmidtke, N Hildebrand, S Wagener and M Holzberger," Infrastrukturkopplung - Platzierung und Betrieb von Ladestationen aus Verkehrs- und Energienetzsicht", *Res electricae Magdeburgenses*; Band 87, 2022
[43] "Navigate methodically into the future with retropolation," WIDIA, [Online]. Available: https://www.maschinenmarkt.vogel.de/mit-retropolation-methodisch-in-die-zukunft-navigieren-gal-408221/?p=. [Accessed 21 September 2021].
[44] M Tayyab, S Helm, I Hauer, J Brinken and N Schmidtke, "Infrastructure linking for placement of Charging stations using Monte Carlo simulation," in 6th IEEE Congress on Information Science, Morroco, 2020.
[45] "Bundesverband der Energie- und Wasserwirtschaft," Meinungsbild E-Mobilität, Berlin, 2019.
[46] Y Zhou, Z Li and X Wu, "The Multiobjective Based Large-Scale Electric Vehicle Charging behaviours Analysis," Complexity, p. 16, 2018.
[47] W Meng and L kai, "Optimization of Electric Vehicle Charging Station Location Based on Game Theory, " in International Conference on Transportation, Mechanical, and Electrical Engineering (TMEE), China, 2011, December 16-18, Changchun, China
[48] L T Nghia, T T Giang, Q H Anh, P T T Binh, N T An and P H Hau, "A voltage sensitivity index application for power system load shedding considering the generator controls," International Journal of Advanced Engineering, vol. 5, no. 12, pp. 618-624, 2019.
[49] S G Naik, D K Khatod and M P Sharma, "Optimal Allocation of Distributed Generation in Distribution System for Loss Reduction," International Proceedings of Computer Science and Information Technology, vol. 28, 2012.
[50] C Ziegler, A Richter, I Hauer, and M Wolter, "Technical Integration of Virtual Power Plants enhanced by Energy Storages into German System Operation with regard to Following the Schedule in Intra-Day," in 53rd International Universities Power Engineering Conference (UPEC), Glasgow Scotland, 2018.
[51] "What will happen to solar panels after their useful lives are over? ", GreenBiz, 11 May 2018. [Online]. Available: https://www.greenbiz.com/article/what-will-happen-solar-panels-after-their-useful-lives-are-over. [Accessed 3 June 2021].
[52] "How Long do Wind Turbines Last?," TWI, [Online]. Available: https://www.twi-global.com/technical-knowledge/faqs/how-long-do-wind-turbines-last#:~:text=A%20good%20quality%2C%20modern%20wind,correct%20maintenance%20procedures%20being%20followed.. [Accessed 5 June 2021].
[53] J Dancker, M Wolter, J Rosberg and E Tsotsas, "Increasing self-sufficiency in a microgrid: integrated vs. non-integrated energy system approach," in 2018 53rd International Universities Power Engineering Conference (UPEC), Glasgow Scotland, 2018.
[54] "Batterietechnologien," RWTH Aachen (IESA), [Online]. Available: http://www.speichermonitoring.de/ueberpvspeicher/batterietechnologien.html. [Accessed 3 March 2021].
[55] A R Espagnet, "Techno-Economic Assessment of Thermal Energy Storage Integration into Low-Temperature District Heating Networks": Thesis, KTH (Heat and Power Technology) Stockholm.
[56] G Glatzmaier, "Developing a Cost Model and Methodology to Estimate Capital Costs for Thermal Energy Storage," NREL, December 2011. [Online]. Available: https://digital.library.unt.edu/ark:/67531/metadc840257/m2/1/high_res_d/1031953.pdf. [Accessed 2 January 2021].

[57] "Fact Sheet | Energy Storage (2019)," EESI (Environmental and Energy study institute), 22 February 2019. [Online]. Available: https://www.eesi.org/papers/view/energy-storage-2019. [Accessed 4 February 2021].
[58] B Lin, R Roche and A Miraoui, "Microgrid sizing with combined evolutionary algorithm and MILP unit commitment," Applied Energy, vol. 188, p. 547–562, 2017.
[59] E Popovski, T Fleiter, H Santos, V Leal and E O Fernandes, "Technical and economic feasibility of sustainable heating and cooling supply options in southern European municipalities-A case study for Matosinhos,," energy, vol. 153, pp. 311-323, 2018.
[60] "Efficiency of Heat Pump and how long it Lasts," aspirationenergy, 22 March 2021. [Online]. Available: https://aspirationenergy.com/how-long-heat-pump-lasts-and-efficiency-of-heat-pump/. [Accessed 12 August 2021].
[61] "Combined Heat And Power," wbdg, 8 March 2016. [Online]. Available: https://www.wbdg.org/resources/combined-heat-and-power-chp. [Accessed 14 September 2021].
[62] "1–10 kW Stationary Combined Heat and Power Systems Status and Technical Potential," NREL, Colorado, 2010.
[63] F K Abo-Elyousr, J M Guerrero and H S Ramadan, "Prospective hydrogen-based microgrid systems for optimal leverage via metaheuristic approaches," Applied Energy, p. 30, 2021.
[64] "Green hydrogen cost reduction: Scaling up electrolyser," IRENA, 2020. [Online]. Available: https://irena.org/-/media/Files/IRENA/Agency/Publication/2020/Dec/IRENA_Green_hydrogen_cost_2020.pdf. [Accessed 12 September 2021].
[65] M Nicholas, "Estimating electric vehicle charging infrastructure costs across major U.S. metropolitan areas," ICCT: International council on clean transportation, 2019.
[66] "What are EV charging stations and how do they work? " GNY, [Online]. Available: https://www.gny.com/products/electric-vehicle-charging-stations. [Accessed 23 July 2021].
[67] J Fleer, S Zurmühlen, J Badeda, P Stenzel, J F Hake and D U Sauer, "Model-based Economic Assessment of Stationary Battery Systems Providing Primary Control Reserve," Energy procedia, vol. 99, pp. 11-24, 2016.
[68] "National Emissions Trading System," German Emissions Trading Authority (DEHSt), Berlin, 2020.
[69] "Greenhouse gas emission intensity of electricity generation in Europe," European Environment Agency, 2019. [Online]. Available: https://www.eea.europa.eu/data-and-maps/indicators/overview-of-the-electricity-production-3/assessment. [Accessed 16 January 2021].
[70] Freie University Berlin Germany, "Open Data (DWD)," Department of Geosciences /Institute of meteorology, 25 July 2017. [Online]. Available: https://www.geo.fu-berlin.de/met/bibliothek/Open-Data-DWD/index.html. [Accessed 2 October 2021].
[71] RWE Npower renewables (Mechanical and Electrical Engineering), "Wind Turbine Power Calculations," [Online]. Available: https://www.raeng.org.uk/publications/other/23-wind-turbine. [Accessed 4 January 2017].
[72] T Lang, D Ammann and B Girod, "Profitability in the absence of subsidies: A techno-economic analysis of rooftop photovoltaic self-consumption in residential and commercial buildings," Renewable Energy, pp. 77-87, 2016.
[73] M Farivar and S H Low, "Branch flow model: Relaxations and convexification—Part I," IEEE Transactions on Power Systems, vol. 28, no. 3, p. 2554–2564, 2013.
[74] M E Baran and F F Wu, "Network reconfiguration in distribution systems for loss reduction and load balancing," IEEE Transactions on Power Delivery, pp. 1401-1407, 1989.
[75] V Kekatos, "DistFlow and LinDistFlow," .faculty.ece.vt.edu, [Online]. Available: https://www.faculty.ece.vt.edu/kekatos/pdsa/Lecture11.pdf. [Accessed 23 November 2021].
[76] Y B Haim, "Info-gap decision theory: decisions under severe uncertainty," Elsevier, 2006.

[77] M Kazemi, B Mohammadi-Ivatloo and M Ehsan, "Risk-constrained strategic bidding of GenCos considering demand response," in IEEE Trans Power System, 2015.
[78] G P McCormick, "Computability of global solutions to factorable non-convex programs: Part 1-Convex understanding problems," Math program, no. 10: 147-75, 1976.
[79] 6.6 Anlage_zur_BV-0033_2015_-_Planzeichnung.pdf, Alte -Zieglei.
[80] "Microgrid," Center for energy and climate solution, [Online]. Available: https://www.c2es.org/content/microgrids/. [Accessed 2 November 2021].
[81] "Mobilität in Deutschland 2008," Feberuary 2008. [Online]. Available: http://www.mobilitaet-in-deutschland.de/pdf/infas_MiD2008_Abschlussbericht_I.pdf. [Accessed 4 July 2019].
[82] Kraftfahrtbundesamt: Neuzulassungen, "Zahlen des Jahres 2020 im Überblick," 2020. [Online]. Available:https://www.kba.de/DE/Statistik/Fahrzeuge/Neuzulassungen/neuzulassungen_node.html. [Accessed 4 September 2021].
[83] E Koptyug, "Number of new car registrations in Germany from 1955 to 2020," Statista, 19 February 2021. [Online]. Available: https://www.statista.com/statistics/587730/new-car-registrations-germany/. [Accessed 05 January 2022].
[84] E Koptyug, "Number of registered cars in Germany from 1960 to 2020," Statista, 26 November 2020. [Online]. Available: https://www.statista.com/statistics/587764/number-of-registered-cars-germany/. [Accessed 02 January 2022].
[85] J Löfberg, "YALMIP: A Toolbox for Modeling and Optimization in MATLAB," in Proceedings of the CACSD Conference, Taipei, Taiwan, 2004.
[86] "ENBREEZE 15 KW WIND TURBINE," ENBREEZE, 2020. [Online]. Available: http://enbreeze.com/en/enbreeze15kw/. [Accessed 10 January 2022].
[87] "Commercially available fuel cell products," US Fuel Cell Council, [Online]. Available: https://www.hydrogen.energy.gov/pdfs/htac_fc_products.pdf. [Accessed 15 January 2022].
[88] T Nowak, "Large scale heat pumps," European heat pump association, [Online]. Available: https://www.ehpa.org/fileadmin/documents/Large_heat_pumps_in_Europe_final.pdf. [Accessed 12 January 2022].

Annex

ALGORITHM: HOLISTIC METHOD FOR MICROGRID PLANNING AND OPERATION

Input: *grid data (e.g., number of persons, loads, lines, nodes, transformer)*
Declaration of input parameters: *planning and operation horizon, scenarios, DERs limits, efficiencies, DERs cost and lifetimes, emission parameters, and so on)*
Allocation of load profiles: *electrical and heat load profiles*
Interpolation: *interpolation of data to match horizons*
Declaration of varaibles: *decision variables (e.g capacities of DERs)*
Integrate e-mobility infrastructure model: *number of EV and EV charging behaviors and number of EVCS and placement nodes of EVCS*
While *(Y<planning horizon)*
  Emissions parameters: *emissions intensity for the grid and certificate cost interpolation*
  While *(T<operation horizon)*
    Solve deterministic optimization problem: *solve for minimization of cost and emission with constraints for DERs model, electrical and heat grid, and energy balance*
    Iteration: *jump to the next time step*
  End
  While *(T<operation horizon)*
    Solve IGDM-based stochastic optimization: *solve for robustness while taking the resulted cost of microgrid from the deterministic optimization problem*
    Iteration: *jump to the next time step*
  End
  Iteration: *jump to the next planning year*
End

ALGORITHM: E-MOBILITY INFRASTRUCTURE

Import the computed number of EV: *retrolpolation method for computation*
While *(Y<planning horizon)*
  While *(T<operation horizon)*
    Set the EVCS variables to zero: *EV_charge, EV_waiting, and EV_charging*
    While *(EV<total number of EVs)*
      Monte –carlo simulation: *do a monte carlo simulation based on the distribution fit and random numbers for EV behaviors*
      While *(EVCS< maximum number of possible EVCS)*
        Compute the occupancy time: *occupancy and waiting time of EVs*
        Iteration: *jump to the next EVCS*
      End
      Iteration: *jump to the next EV*
    End
    Iteration: *jump to the next time step*
  End
  Iteration: *jump to the next planning horizon*
End
EVCS placement algorithm*: run the monte-carlo simulation to the placement of EVCS*

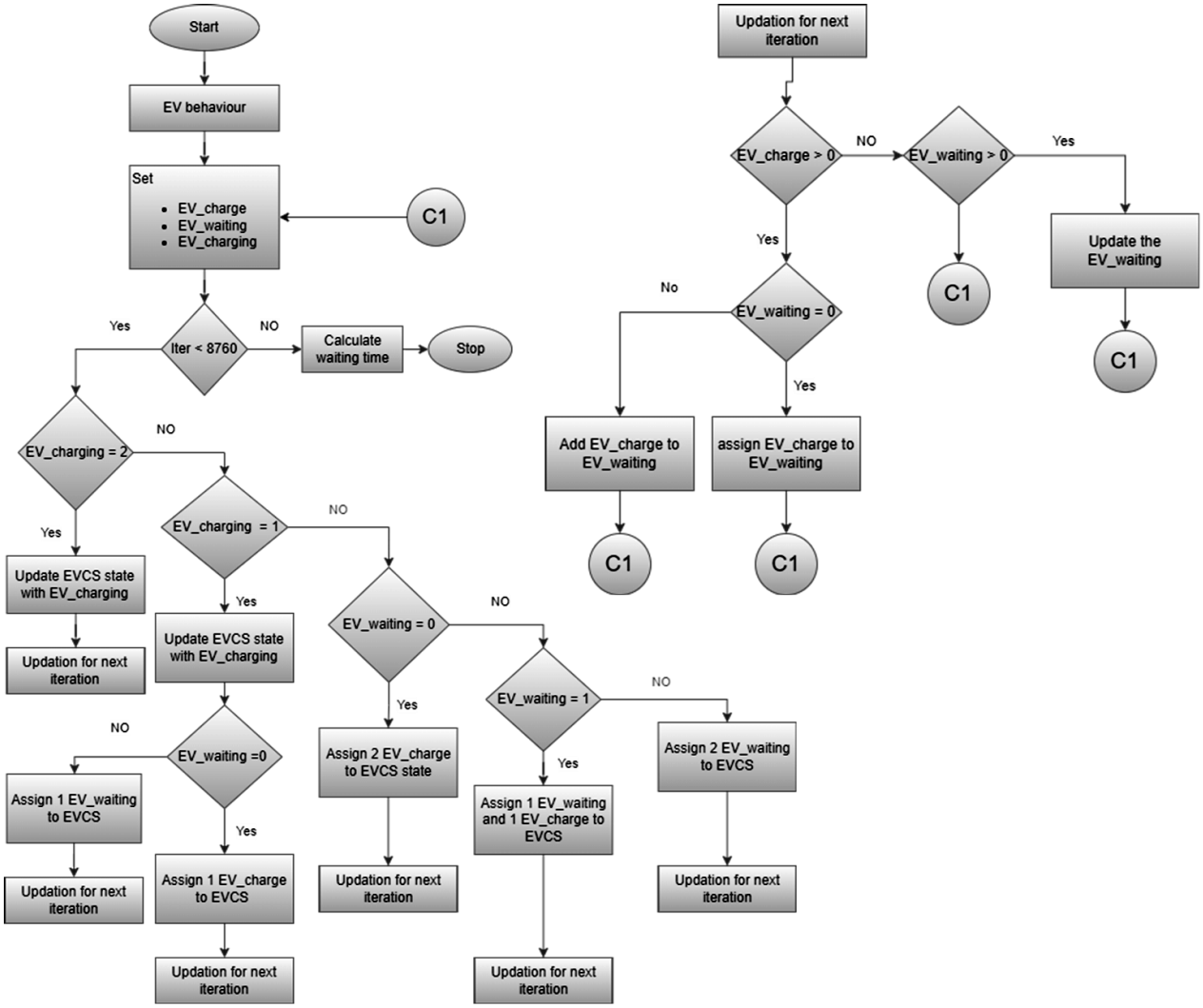

Figure A1 Method for calculation of occupancy time

The EV has three states charged, waiting, or queuing for charging. Three variables represent the three states. EV_charge variable holds the ID of EVs that require charging, $EV\_charging$ variable holds the ID of EVs already charging at the charging station, and the $EV\_waiting$ variable has the ID of EVs in the waiting queue from the previous time step. After setting those variables at the start of the iteration, the $EV\_charging$ state is checked first, as shown in figure A1 (left). If two EVs are charging, then the EVs arriving at that time are added to the waiting queue. If there is one EV charging, one slot is empty and is assigned from the waiting queue, if any, or from the EVs arriving at that time. After setting the EVs to an empty slot, updating variables for the next step is done, as shown in figure A1 (right). If there are no EVs charging, then two slots are empty, and already waiting EVs are given priority, and if there are any left, then EVs arriving at that time step are assigned.